ORNL-3098
UC-37 – Instruments

THE DEVELOPMENT OF A DIRECT COUPLED, TRANSISTORIZED, SUB-MILLIMICROAMPERE CURRENT AMPLIFIER

F. T. May

OAK RIDGE NATIONAL LABORATORY

operated by

UNION CARBIDE CORPORATION

for the

U.S. ATOMIC ENERGY COMMISSION

DISCLAIMER

Printed in USA. Price $2.50. Available from the
Office of Technical Services
Department of Commerce
Washington 25, D.C.

ORNL-3098

Contract No. W-7405-eng-26

THERMONUCLEAR DIVISION

THE DEVELOPMENT OF A DIRECT COUPLED, TRANSISTORIZED, SUB-MILLIMICROAMPERE CURRENT AMPLIFIER

F. T. May

DATE ISSUED

AUG 11 1961

Submitted as a Thesis to the Graduate Council of the University of Tennessee in partial fulfillment of the requirements for the degree of Master of Science

OAK RIDGE NATIONAL LABORATORY
Oak Ridge, Tennessee
operated by
UNION CARBIDE CORPORATION
for the
U.S. ATOMIC ENERGY COMMISSION

ACKNOWLEDGEMENT

The author wishes to express sincere appreciation to the members of the Thermonuclear Division of the Oak Ridge National Laboratory who gave encouragement and assistance in the work described in this thesis; to Professors J. F. Pierce and G. W. Hoffman for helpful suggestions pertaining to the final organization and form; and to my wife, Darlene, and Charlotte Rose for their competent typing of the manuscript. Special gratitude is due R. A. Dandl, head of the Diagnostics Group of the Thermonuclear Division, who first observed the high gain effect and gave many suggestions that aided in the amplifier design, and Mendel Maskewitz who helped build the test equipment and take the data.

TABLE OF CONTENTS

INTRODUCTION

Due to a very unusual effect[1] that occured when certain transistors were operated with low collector current, a direct coupled, transistorized, current amplifier has been developed with sensitivities extending below the millimicroampere region of input currents. This amplifier employed shunt feedback and exhibited very reproducible characteristics. The sequence of events leading up to the discovery of the special effect and the design and testing considerations employed in the incorporation of the transistors into the amplifier are presented in the following thesis.

A NEED FOR LOW CURRENT MEASUREMENTS

In order to study certain characteristics of the experimental controlled fusion machine, DCX (Direct Current Experiment)[2], it was necessary to measure currents[3] at the millimicroampere level and higher. The instruments used for such measurements had to be stable d-c devices, relatively free of noise, capable of operating in a magnetic field, relatively free of microphonic pickup, capable of driving recording devices, equipped with a wide range of sensitivities with reasonable bandwidths, easy to maintain, and portable.

INITIAL CURRENT AMPLIFIERS

For some time these requirements have been filled by shunt fedback , transistorized, direct coupled, current amplifiers. Transistors were preferred mainly because of high magnetic field environments. The first amplifier design (Figure 1) used for this purpose employed a Philco PNP, germanium, surface barrier 2N346 as the input transistor. This amplifier was limited by stability and noise for currents below 10^{-7} amp. A second amplifier (Figure 2) with improved characteristics was designed using a Transitron NPN, silicon, 2N1247 as the input transistor. This transistor was especially designed for low noise input applications and allowed for operation extending into the millimicroampere range.

Table I shows the characteristics of these two amplifiers. The sensitivity is defined in terms of the input current required for an output of one volt. The equivalent input noise was easily determined by noting the output noise voltage and correcting by the sensitivity to refer this value to an equivalent input current. For example, a rms (root mean square) output noise level of 2×10^{-3} volts with a sensitivity of $1/10^{-6}$ volt/amp would result from an equivalent rms input noise current of 2×10^{-9} amp.

The risetime was expressed as an important characteristic since it clearly indicated the speed with which the amplifiers could respond to an input current. The specific application for which these amplifiers were designed involved primarily the measurement of an input current that would maintain some d-c level and then, when desired, would decay with time constants of the order of one millisecond or greater. The response of the amplifiers was clearly fast enough to follow such transients.

The limit of usefulness of any amplifier when used in a feedback configuration is determined from the d-c drift, response time,

UNCLASSIFIED
ORNL-LR-DWG. 56720

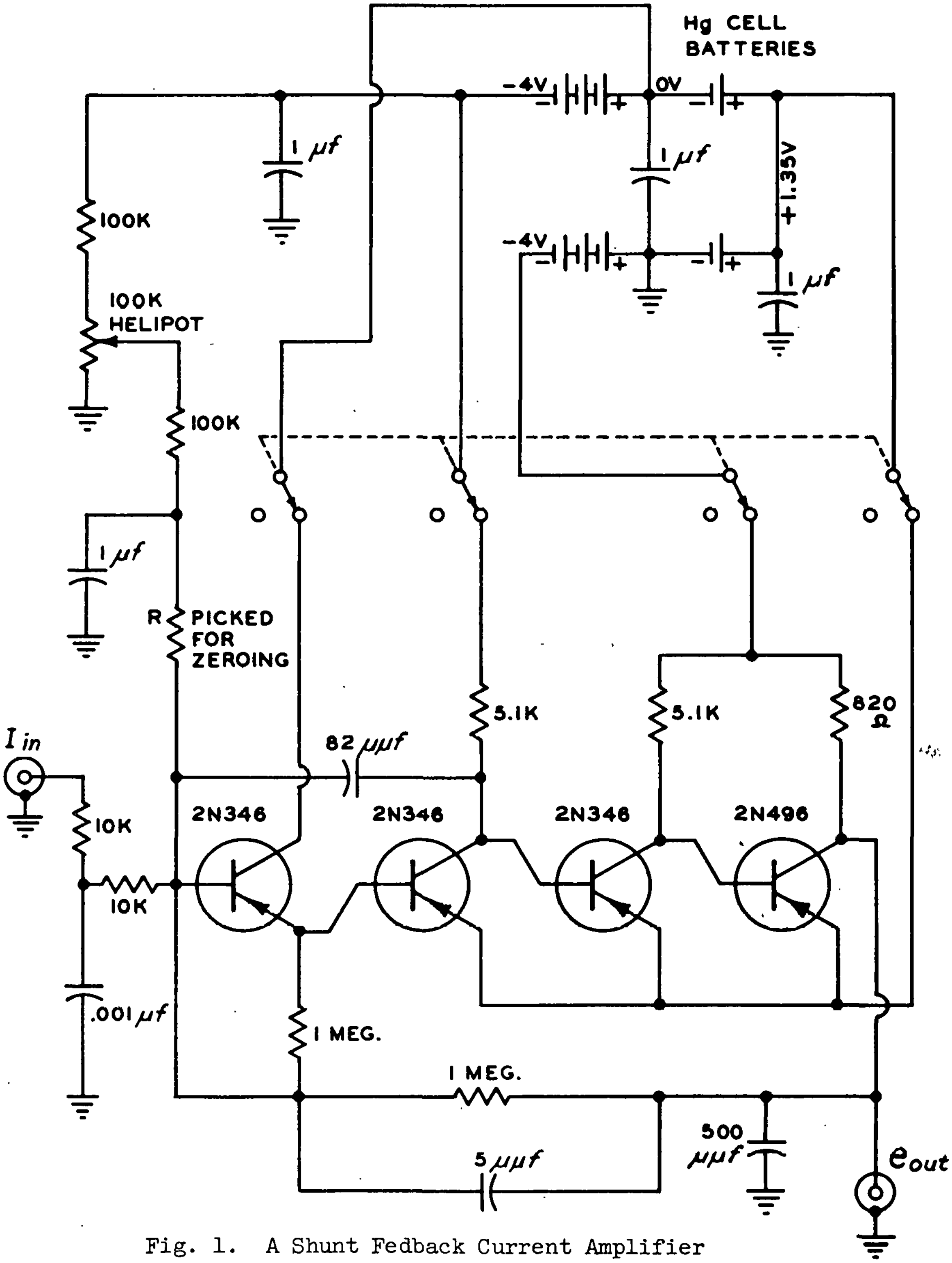

Fig. 1. A Shunt Fedback Current Amplifier With a Sensitivity of $\frac{1}{10^{-6}}$ $\frac{\text{volt}}{\text{amp}}$

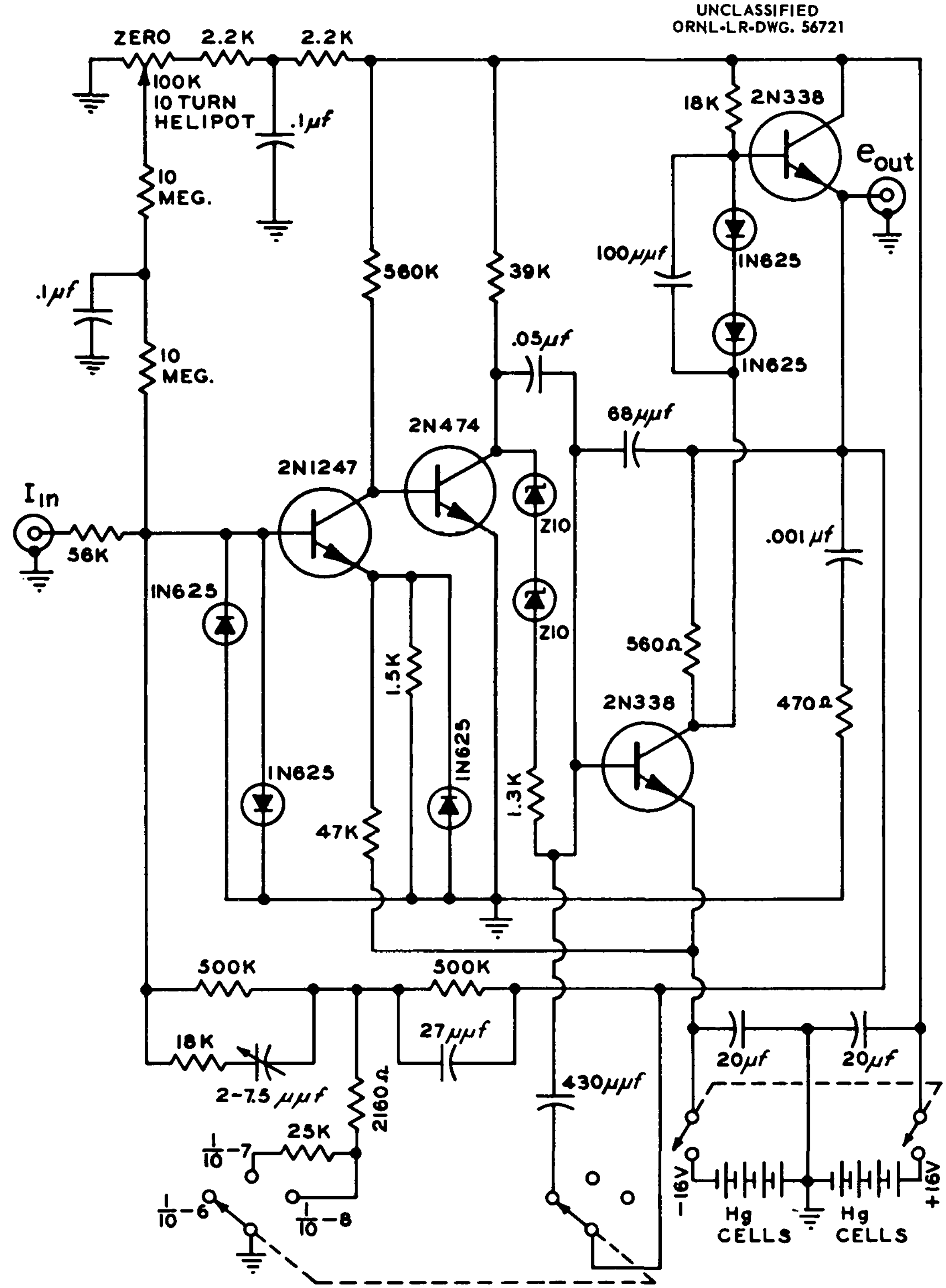

Fig. 2. A Shunt Fedback Current Amplifier With Sensitivities of $\frac{1}{10^{-6}}$, $\frac{1}{10^{-7}}$, and $\frac{1}{10^{-8}}$ $\frac{\text{volt}}{\text{amp}}$

Table I. Characteristics of the Amplifiers
Shown in Figures 1 and 2

Amplifier	Sensitivity	rms Noise Referred to a Current Input	Risetime	Output Dynamic Range	d-c Drift Referred to a Current Input
	$\frac{\text{volt}}{\text{amp}}$	amp	μsec	volts	$\frac{\text{amp}}{\text{min}}$
No. 1	$\frac{1}{10^{-6}}$	7×10^{-10}	3	+1.35 to -4	$\frac{10^{-8}}{10}$
No. 2	$\frac{1}{10^{-6}}$	7×10^{-10}	10	-16 to +16	$\frac{4 \times 10^{-10}}{10}$
No. 2	$\frac{1}{10^{-7}}$	3.5×10^{-10}	25	-16 to +16	$\frac{4 \times 10^{-10}}{10}$
No. 2	$\frac{1}{10^{-8}}$	1.4×10^{-10}	50	-16 to +16	$\frac{3 \times 10^{-10}}{10}$

noise level, and sensitivity. It is evident that the second amplifier was definitely superior to the first under these considerations. Also the improved dynamic range of the output voltage permitted a wider range of input signals without experiencing saturation effects. Further elaboration on a criteria for design of shunt feedback current amplifiers with special emphasis on transitor amplifiers follows in a later section.

Although the second amplifier filled the requirements of most currents that needed to be measured, it was desirable to have amplifiers with even more sensitivity for proposed experiments on DCX and associated machines. The fact that the usual sacrifice of decreased bandwidth (increased risetime) for greater sensitivity had to be made was conveniently offset by the characteristics of the DCX current that should decay slower when the total current was smaller. However to go to smaller input currents input transistors with reasonable gain for currents below 10^{-9} amp were required. A thorough study of the manufacturers' specifications of commercially available transistors failed to reveal any transitor that was an improvement over the 2N1247 used in the second amplifier. (This was in the Fall of 1959).

TESTING TRANSISTORS FOR GAIN AT LOW BASE CURRENTS

At this time a study of all available transistors was initiated to determine their respective gains to input currents below a microamp. A modified diagram of the type of test circuit used to study the transistors is shown in Figure 3. This circuit was well shielded and care was taken to properly mount the large resistors in the base circuit. The collector current was measured with a very stable d-c micro-microampere meter that required a negligible voltage drop. The method of measuring the current gain was to note the change of collector current, ΔI_c, with a ten per cent change in the base current, ΔI_b. The base current was approximately $\frac{5}{R_b}$ amp and the ten per cent change resulted from the action of the microswitch. The bucking current adjustment allowed for the observation of small collector current changes in the presence of larger collector currents. This, of course, gave a d-c current gain of Beta = $\frac{\Delta I_c}{\Delta I_b}$ by definition.

Most all transistors failed to have any current gain when the base currents were below 10^{-7} amp and many failed to show any gain with base currents of 10^{-6} amp. In the normal regions of operation, of course, all of the transistors met the manufacturers' specifications. This behavior is typical for modern junction transistors and the variation of current gain with emitter current

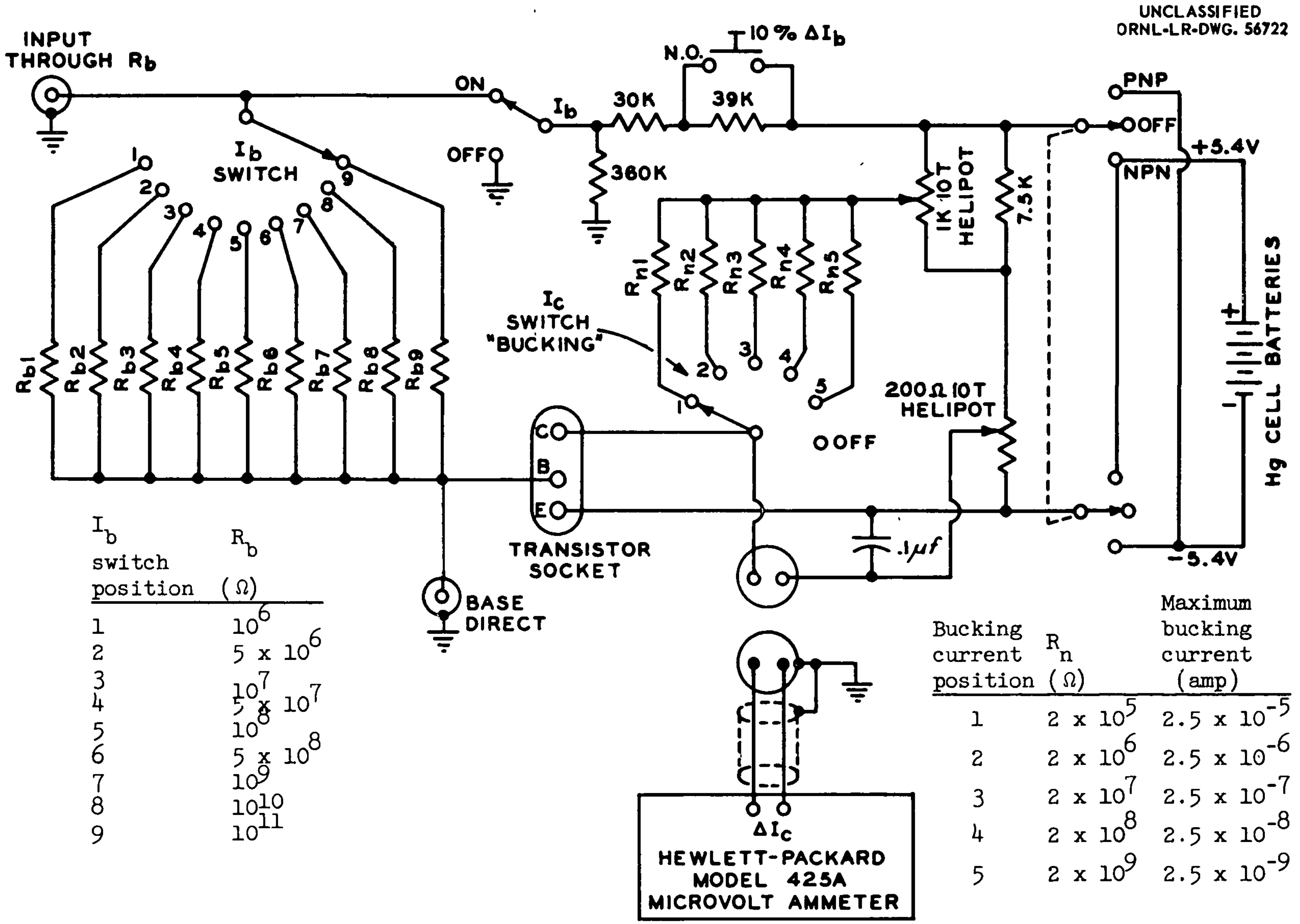

I_b switch position	R_b (Ω)
1	10^6
2	5×10^6
3	10^7
4	5×10^7
5	10^8
6	5×10^8
7	10^9
8	10^{10}
9	10^{11}

Bucking current position	R_n (Ω)	Maximum bucking current (amp)
1	2×10^5	2.5×10^{-5}
2	2×10^6	2.5×10^{-6}
3	2×10^7	2.5×10^{-7}
4	2×10^8	2.5×10^{-8}
5	2×10^9	2.5×10^{-9}

Fig. 3. Low Current d-c Beta Tester

has been explained theoretically.[4] Since the emitter current is set by the base current, the theory can be thought of in terms of base current which was of interest in this study.

The first transistor that revealed interesting properties in the region below a microamp was the General Electric, NPN, germanium, alloy junction, 2N167. This transistor and the previously mentioned 2N346 have been two of the best germanium types used in our low current applications in the microamp region of input currents.

FIRST OBSERVATION OF VERY UNUSUAL EFFECT

In the middle of December 1959, R. A. Dandl was testing some transistors with the special tester and found a Texas Instruments 2N338 that exhibited characteristics that were completely different from any other type previously tested. This transistor yielded a current gain of approximately 40,000 with a base current of 5×10^{-11} amp. The observation of this unusual effect immediately brought about a complete study of a number of 2N338's and also a number of 2N336's that were found to exhibit the same effect. These were NPN, grown-diffused, silicon transistors.

SPECIAL TRANSISTOR CHARACTERISTICS

Some of the data taken on these two transistor types has been published.[1] The following presentation, however, is much more detailed and is directed toward the actual utilization of the transistors in current amplifiers.

COLLECTOR CURRENT AND CURRENT GAIN

One set of data that was very indicative of the characteristics of the transistors of interest is presented in Figures 4 and 5. This data, in the form of log-log plots, shows the dependence of collector current and current gain on the base current. The curves describe the behavior of three 2N338 and three 2N336 transistors and they clearly show the tremendous variations that occurred in the millimicroampere region of base currents. It should be stated here, however, that the characteristics of each individual transistor were very reproducible and that all of the transistors met the manufacturers' specifications in the normal regions of operating currents. These data were taken with a collector-to-emitter voltage, V_{ce}, of +0.5 volt. The current designated as I_{ceo} was the "leakage" collector current that existed when V_{ce} was applied with no base current. This will be referred to as the "floating base" condition.

It has been noted that the transistors that had the unusual amplification properties also exhibited the largest "leakage" currents in the "floating base" condition. This can be seen by comparing the transistor "leakage" currents of Figure 4 to the respective

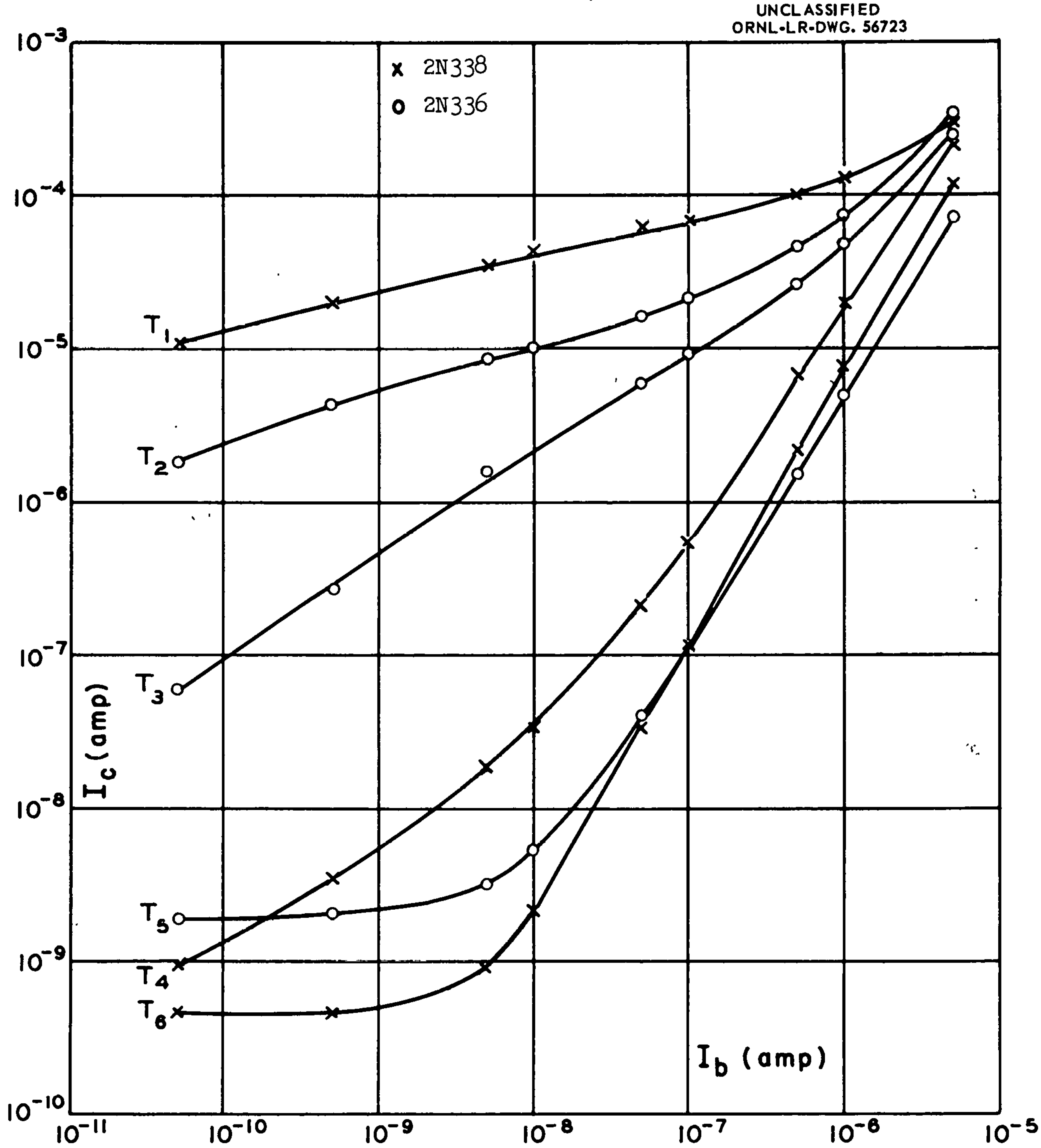

Transistor	T_1	T_2	T_3	T_4	T_5	T_6
I_{ceo}($\times 10^{-6}$ amp)	9.0	9.4×10^{-1}	2.2×10^{-2}	5×10^{-4}	1.9×10^{-3}	4.6×10^{-4}

Fig. 4. Collector Current and Base Current Relation of a Number of Texas Instruments 2N336 and 2N338 Transistors. (V_{ce} = +0.5 volt)

UNCLASSIFIED
ORNL-LR-DWG. 56724

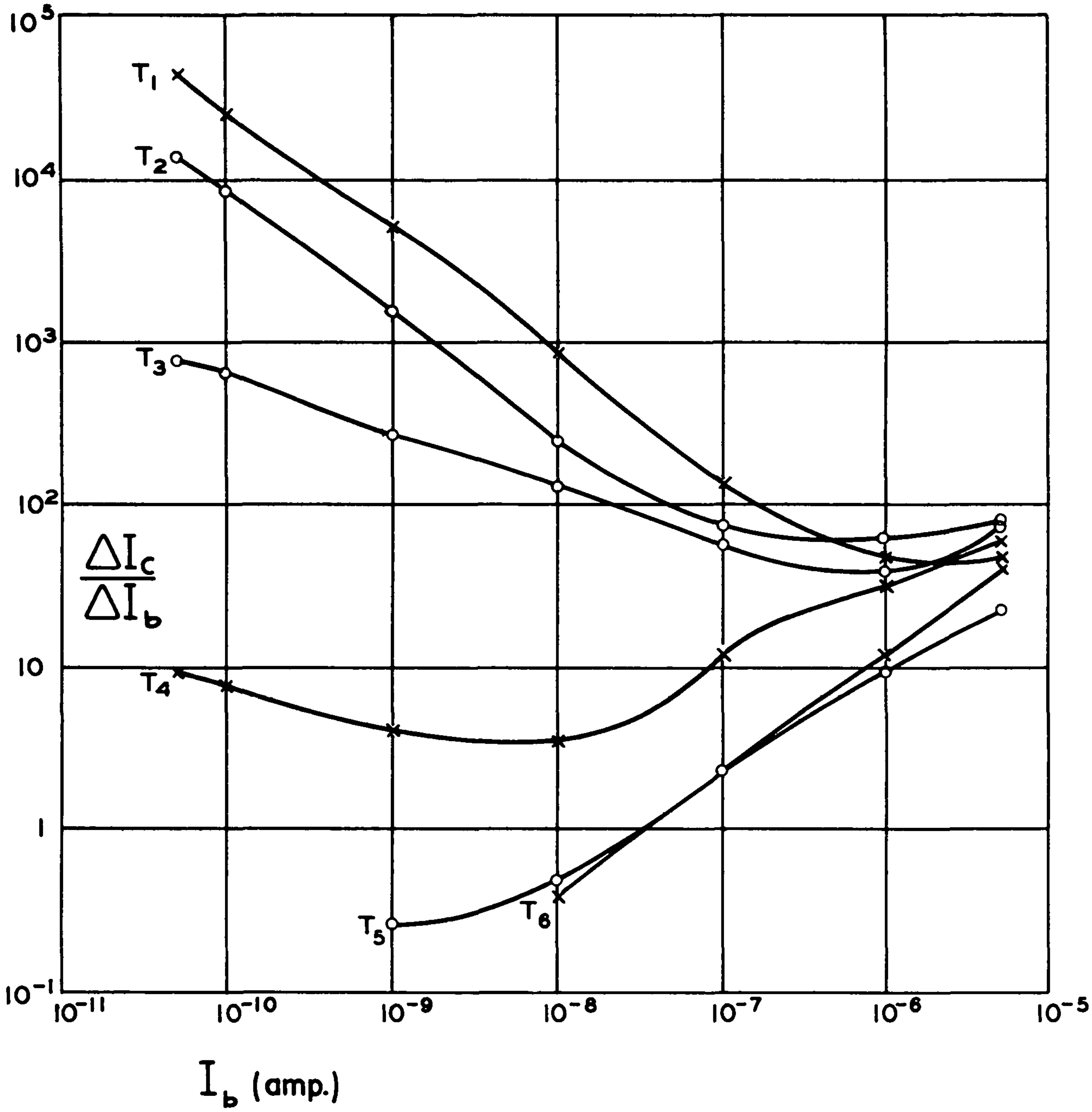

Fig. 5. D-C Beta and Base Current Relation of the Transistors referred to in Fig. 4

current gain curves of Figure 5. For example, the transistor that had the largest "leakage" current was T_1 with an I_{ceo} of 9 microamps. This same transistor consistently demonstrated the highest current gain of the group in the region below 5×10^{-7} amp of base current.

Another interesting observation that was evident from Figure 5 was that the transistors of real interest, T_1, T_2, and T_3, had fairly constant slopes on the log-log plot in the region of lower base currents showing an inverse type of relation between current gain and base current over a range of three or four decades. This very radically departed from the behavior of any other types tested. Figures 4 and 5 also serve to illustrate this since it can be said that transistors T_5 and T_6 represent the behavior of the majority of the other types of transistors tested. Many failed to give curves even as good as these. Because of the possible interest of studying faster transistors, data on some with the mesa type of construction are presented in Appendix I. The ones that proved most interesting behaved similar to or better than T_4.

CURRENT GAIN SPREAD

The current amplification spread, with $I_b = 5 \times 10^{-11}$ amp, $V_{ce} = +0.5$ volt, of all of the Texas Instruments 2N336 and 2N338 units that were tested up to April 20, 1960, is shown in Table II. From the table it was obvious that the percentage with gains greater than 1000 was certainly large enough to produce a satisfactory yield of high gain transistors for experimental purposes from a relatively small order. Also it indicated that the yield might be higher from the 2N336 units. It should be stated here that the Texas Instruments transistors proved to have the best high gain behavior. However, due to a new manufacturing procedure begun in August 1960, the existence of the high gain effect seems to have been altered. Eighteen transistors bought since then were tested and only one had any interesting gain and that was only 200 with $I_b = 5 \times 10^{-11}$ amp, $V_{ce} = 1.0$ volt. Twelve General Electric 2N338 transistors were tested with absolutely no success below 10^{-7} amp of base current. From a group of twelve Transitron 2N338 units five had a gain greater than twenty at $I_b = 5 \times 10^{-10}$ amp, $V_{ce} = +0.5$ volt. Table III shows this beta spread. All of the following amplifier applications employed only Texas Instruments transistors for the inputs.

COMMON EMITTER CHARACTERISTIC CURVES

A more familiar presentation of the common-emitter characteristics of a high gain 2N336 is shown in Figure 6. The current gain at $I_b = 5 \times 10^{-11}$ amp, $V_{ce} = +0.5$ volt, was 3000. This plot shows the collector current versus collector-to-emitter voltage behavior with the base current as a parameter. The only departure from standard curves was the low base currents that, of course, caused the low collector currents. Notice that saturation occurred at the voltage that is characteristic of all silicon transistors in the normal range of operating currents. Also, an

Table II. Distribution of the d-c Current Gain of all Texas Instruments 2N338 and 2N336 Transistors Tested up to April 20, 1960. ($I_b = 5 \times 10^{-11}$ amp, $V_{ce} = +0.5$ volt)

$\frac{\Delta I_c}{\Delta I_b}$	0 to 1	1 to 100	100 to 1000	1000 to 10,000	greater than 10,000
2N338	11	20	2	1	3
2N336	14	10	26	9	5

Table III. Distribution of the d-c Current Gain of Twelve Transitron 2N338 Transistors. ($I_b = 5 \times 10^{-10}$ amp, $V_{ce} = +0.5$ volt)

$\frac{\Delta I_c}{\Delta I_b}$	0 to 1	20	80	300	480
2N338	7	2	1	1	1

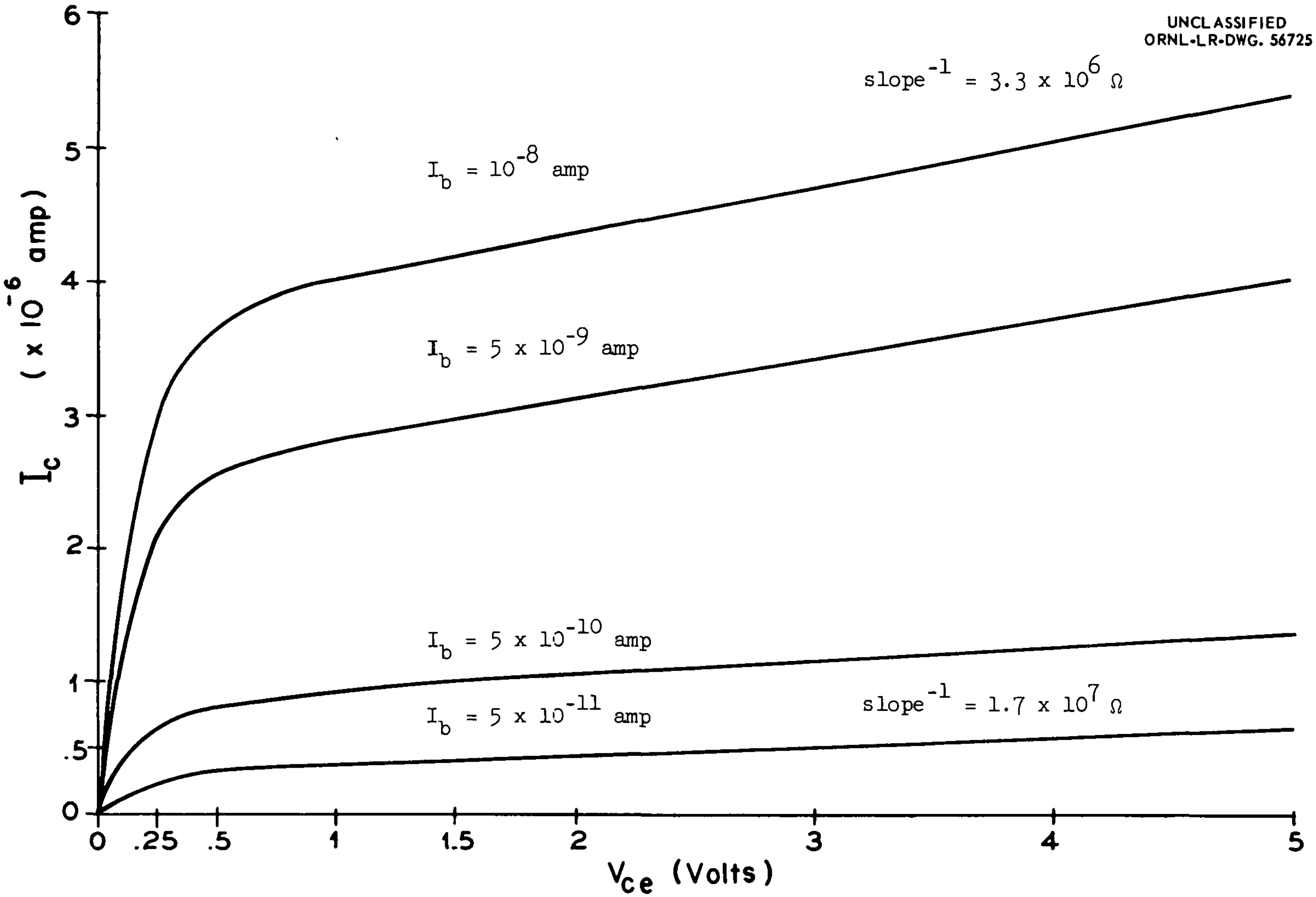

Fig. 6. Common-Emitter Characteristic Curves of a Texas Instruments 2N336 Transistor. (Beta = 3000 at $I_b = 5 \times 10^{-11}$ amp, V_{ce} = +0.5 volt)

indication of the collector resistance could be taken from the slopes of the curves giving values ranging from 3.3×10^6 ohms with $I_b = 10^{-8}$ amp to 1.7×10^7 ohms with $I_b = 5 \times 10^{-11}$ amp.

TEMPERATURE DEPENDENCE

The temperature dependence of the current gain and I_{ceo} of a high gain 2N336 is shown in Figure 7. It is interesting to note that the form of these variations was quite similar to the usual temperature characteristics of transistors operating at more conventional current levels.[5]

NOISE

A rough measure of a noise figure can be inferred from a value of 1.2×10^{-4} volts rms noise across a collector resistance of 5×10^6 ohms shunted by 45 uuf. This measurement was made at room temperature on a 2N336 having a current gain of 4200 at $I_b = 5 \times 10^{-10}$, $V_{ce} = +0.5$ volt.

INPUT IMPEDANCE MEASUREMENTS

A knowledge of an equivalent input impedance was of primary importance to the amplifier design and analysis. The assumed form of an equivalent input configuration was a simple parallel R-C network from base to emitter. This impedance, of course, was simply from the input to ground in the common-emitter configuration that was employed for the amplifier inputs that are discussed in detail in a later section.

One measurement of the input resistance, described in

UNCLASSIFIED
ORNL-LR-DWG. 56726

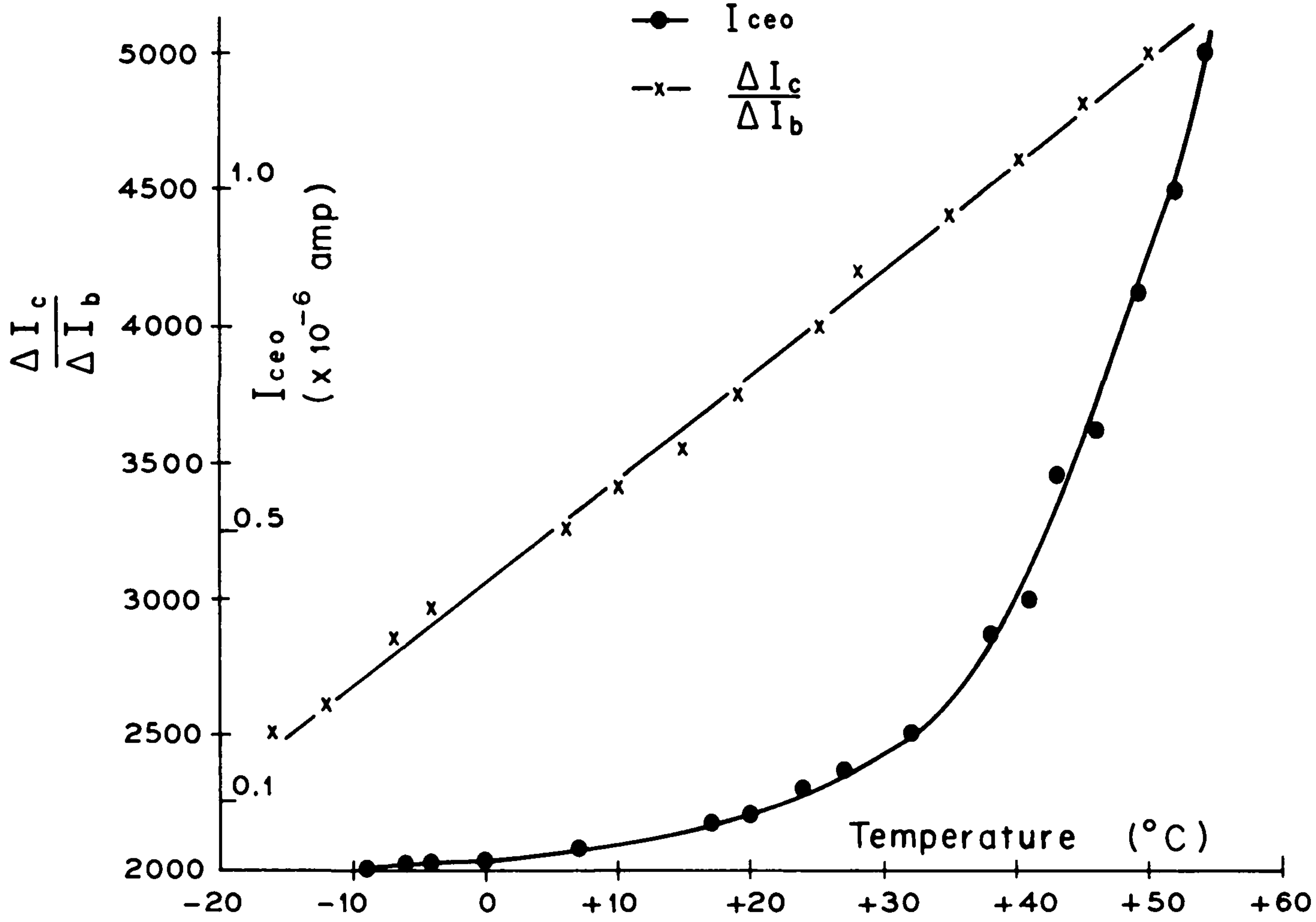

Fig. 7. Temperature Dependence of Beta and I_{ceo} in a High Gain 2N336. (I_b = 5 x 10^{-11} amp, V_{ce} = +0.5 volt)

Appendix II, utilized a simple procedure with a potentiometer and the special transistor tester of Figure 3. Using this technique, an input resistance, R_p, of 3.5×10^9 ohms has been measured with $I_b = 1.4 \times 10^{-11}$ amp (the beta at that current was approximately 20,000). It has been noted that in general the input resistance was highest in the transistors that exhibited the highest respective betas when operating in the millimicroampere region. Some data on the variation of input resistance with input current of two transistors is shown graphically in Figure 8. The increase of input resistance with decreasing current levels was expected. [5]

Another measurement of the input characteristics was made with a commercial capacitance, D - Q, bridge. To do this the Beta tester circuit had to be changed slightly to allow proper shielding of the bridge connections. The bridge was simply coupled into the base with a 0.01 μf capacitor and the tester was operated in the normal fashion to set the d-c conditions for the series of measurements. The bridge generator was set at one kilocycle with a peak-to-peak voltage of fifty millivolts. This magnitude was sufficient for the bridge detector and also seemed reasonable since, from the previous measurements, V_{be} was around one hundred millivolts. With the bridge properly nulled the input capacity, C_p, and resistance, R_p, of the two transistors previously measured was determined using the standard equations relating D, Q, C_s(series), C_p (parallel), and R_p (parallel). The variation of C_p and R_p with I_b is shown graphically in Figure 9. The values of R_p using the static potentiometer measurements were consistently higher than the respective dynamic values calculated from the bridge measurements. This difference probably arose from the simple equivalent input configuration assumed for the transistors. Other more complex input circuits could be assumed to allow for the difference in d-c and a-c measurements, but they would also tend to complicate further analysis with probably no real advantages.

MORE EXPERIMENTS ON THE VARIATION OF CURRENT GAIN

Further study of the operating conditions affecting the high beta effect was made to provide additional data that might aid in arriving at a satisfactory explanation. These experiments took the test transistors to a number of extremes.

Dependence on Collector-to-Base Voltage

An interesting set of data (Table IV) was taken to note the variation of beta as the collector-to-base voltage was varied. This was accomplished by simply controlling the collector-to-emitter voltage allowing the base potential to establish its own level. It is clearly evident from the data that a relatively high collector-to-base potential was not necessary to insure a high current gain since a gain of 6,000 was noted with V_{cb} equal to only 7 millivolts. A decrease of Beta as V_{cb} approached zero was expected since it is a typical characteristic that has been noted in special applications.[6]

UNCLASSIFIED
ORNL-LR-DWG. 56727

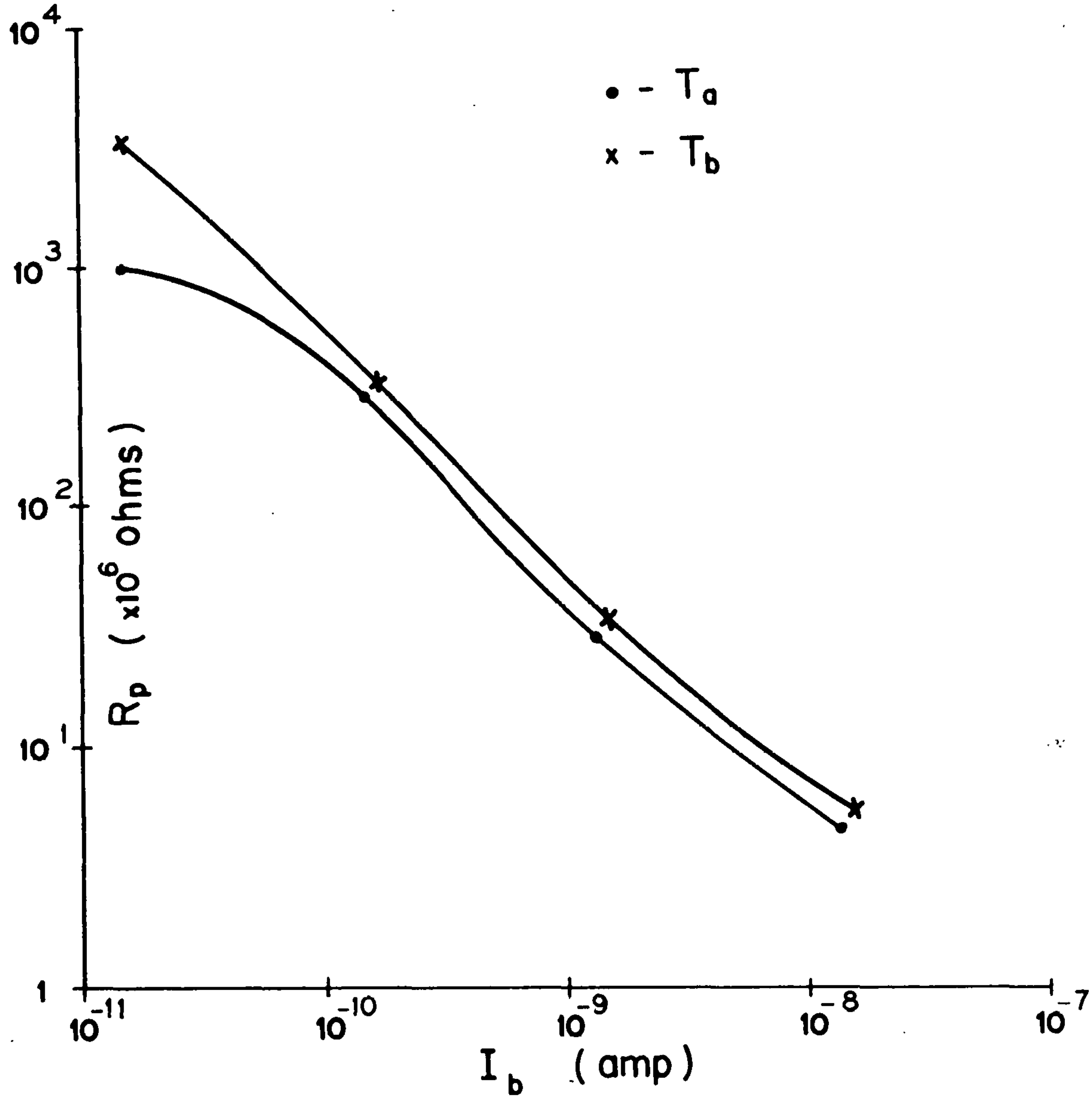

Fig. 8. Variation of Input Resistance with Base Current in Two 2N336 Transistors from Potentiometer Measurements. (Beta of T_a = 1000 and Beta of T_b = 20,000 at $I_b = 5 \times 10^{-11}$ amp, V_{ce} = +1.0 volt)

UNCLASSIFIED
ORNL-LR-DWG. 56728

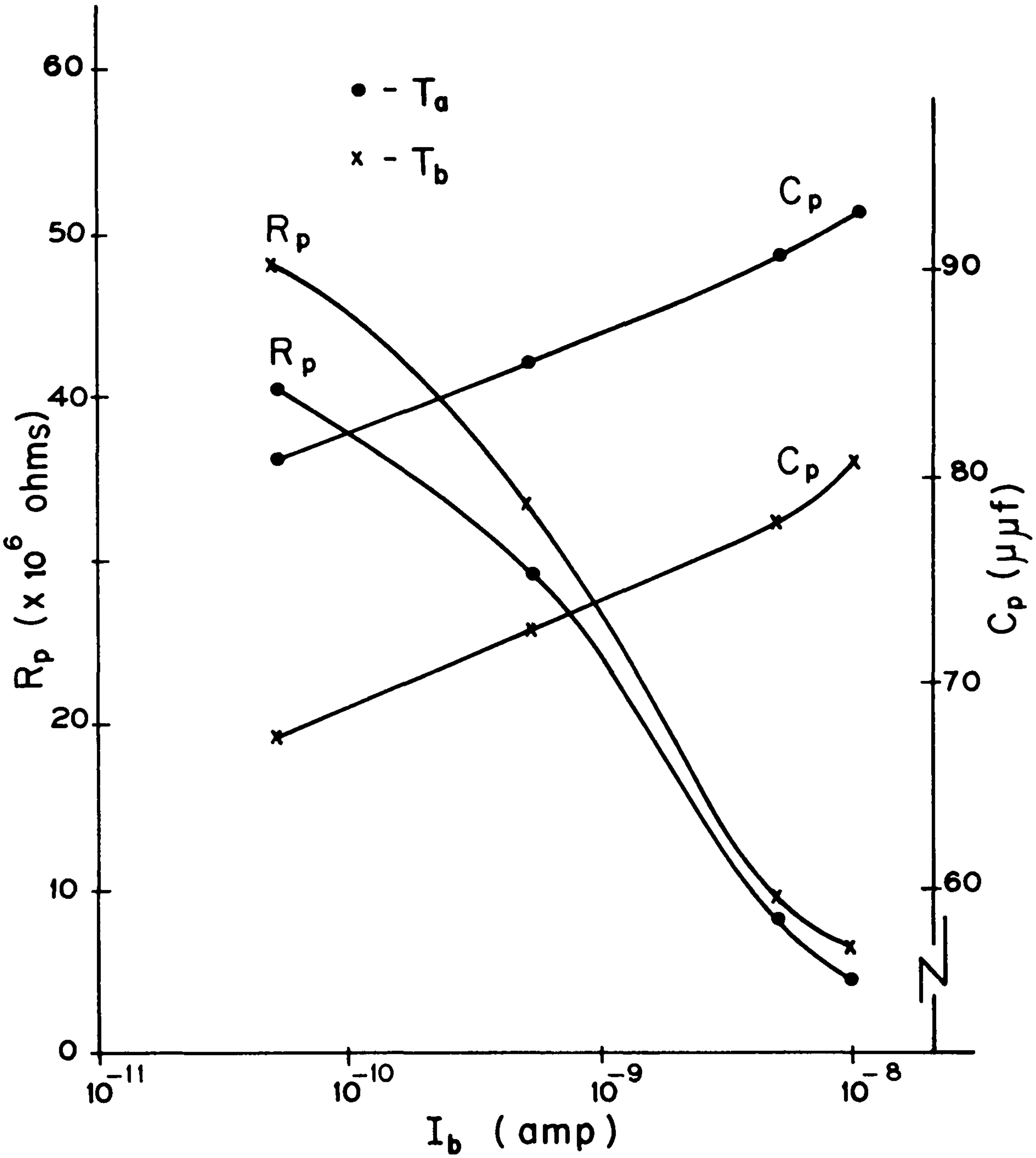

Fig. 9. Variation of Input Resistance and Capacitance with Base Current of the Transistors Referred to in Fig. 8 from Measurements Made with a Commercial Capacitance D-Q Bridge

Effect of Increasing Collector-to-Emitter Voltage

The data of Figures 4 and 5 revealed an apparent relation between the value of the "leakage current", I_{ceo}, and Beta. One approach at a further study of this behavior was made by increasing V_{ce} so that I_{ceo} increased and the corresponding Beta was measured. The curve of Figure 10 resulted and again showed that the two parameters do tend to increase together. However, the undesirable effect of increased basic noise nullified any real advantage from this technique. The signal-to-noise ratio of the transistor actually decreased by roughly an order of magnitude as V_{ce} was increased from 1 to 25 volts. When V_{ce} was increased to 30 volts, the noise was so severe that the value of Beta could not be determined. In transistors that already had Betas greater than 10,000 with V_{ce} equal to approximately 1 volt, the technique proved even worse since the noise went up quite fast while the current gain hardly increased at all. From this data it can probably be safely stated that the optimum value of V_{ce} was in the range from +0.5 to +1.0 volt.

Relation Between Base-to-Emitter Voltage and Collector Current

A simple d-c experiment was performed to see if there was any unusual relation between the base-to-emitter voltage, V_{be}, and I_c. This was done to see if any interesting analogy to a vacuum tube transconductance, g_m, could be inferred, perhaps even to the extent of saying a simple electric field effect action was present. The results are plotted in Figure 11 on a semilog scale

UNCLASSIFIED
ORNL-LR-DWG. 56729

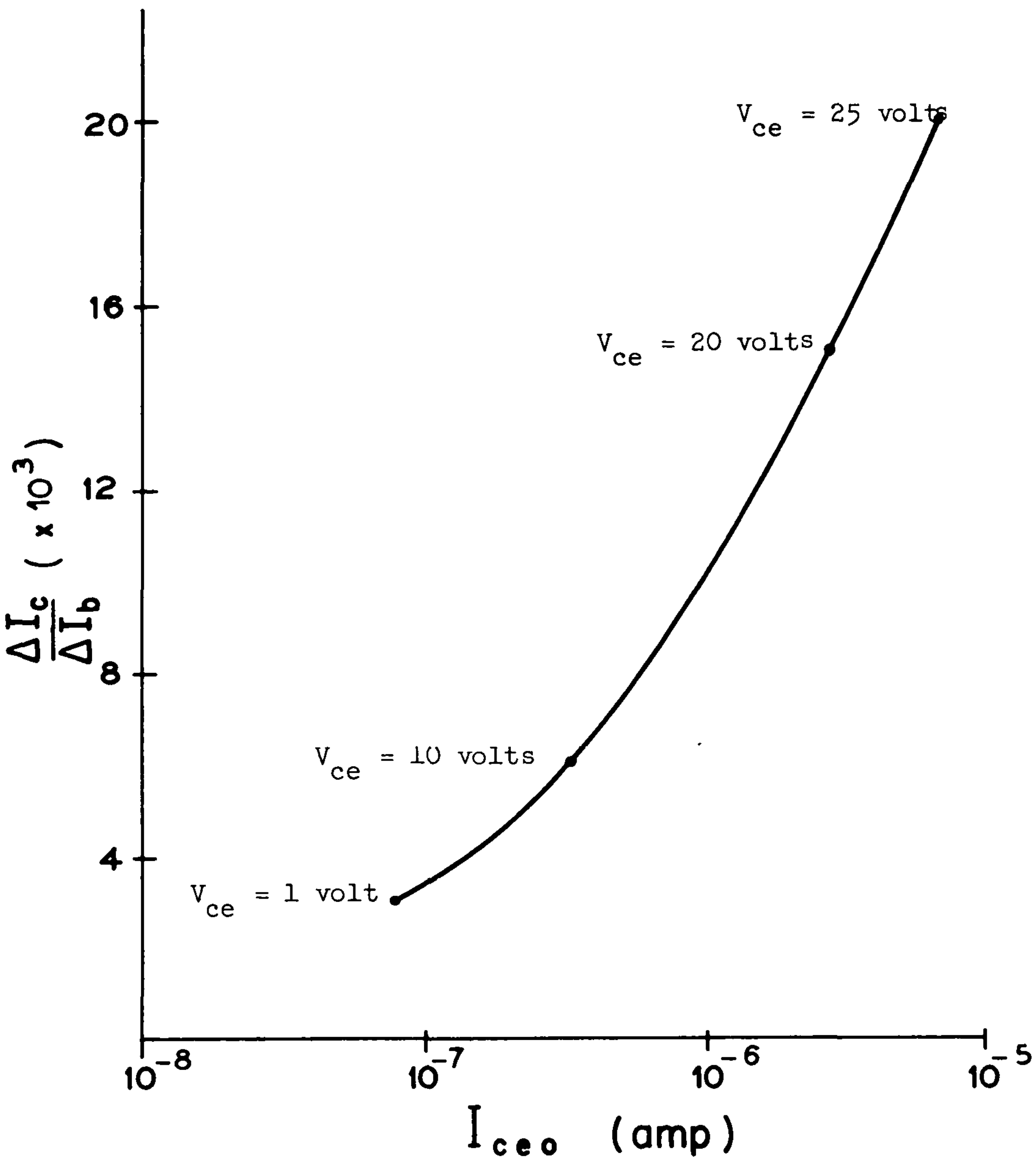

Fig. 10. Relation Between Beta and I_{ceo} Using V_{ce} to Vary the Test Conditions

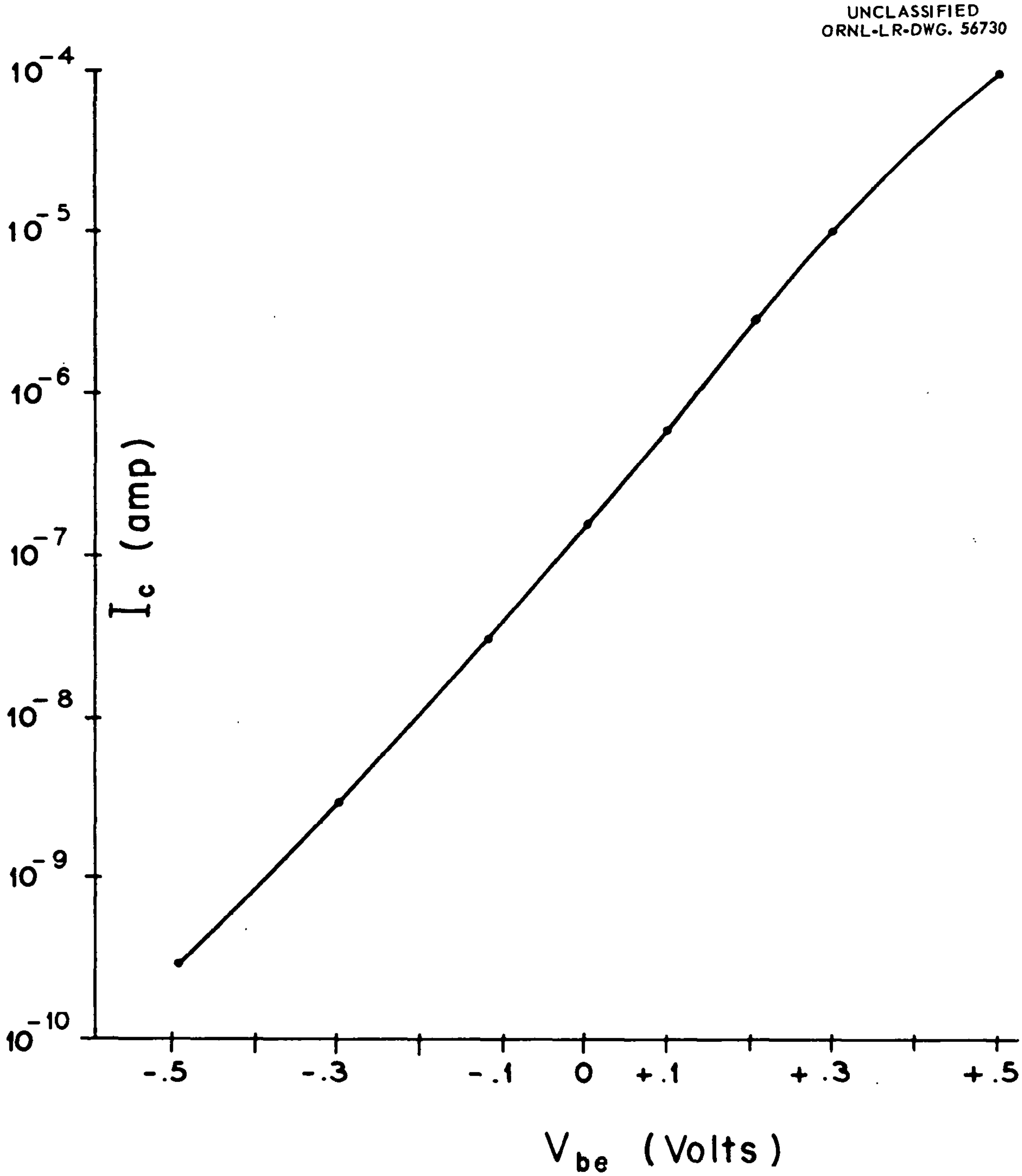

Fig. 11. Dependence of Collector Current on the Base-to-Emitter Voltage. (Beta = 17,000 at $I_b = 5 \times 10^{-11}$ amp, $V_{ce} = +1.0$ volt)

showing an exponential relation with a slope indicating a $g_m = 6$ micromhos in the region of V_{be} around 50 millivolts. A consideration of Beta and the input resistance, R_p, of course, could be used to arrive at a g_m expression simply by the definition

$$g_m = \frac{\Delta I_c}{\Delta V_{be}} = \frac{\beta \Delta I_b}{\Delta V_{be}} = \frac{\beta}{R_p} \text{ micromhos} \tag{1}$$

Using d-c terms already presented in Figure 8 a calculated g_m would be

$$g_m = \frac{\text{Beta}}{R_p} = \frac{2 \times 10^4}{3.5 \times 10^9} = 5.7 \text{ micromhos}$$

in the region of high low-current sensitivity. (A good standard electrometer tube, CK5886, has a g_m of 40 micromhos with a much higher input resistance).

<u>Relation Between "Floating Base" Potential and High Gain</u>

Data were also taken to note the respective values of the "floating base" potential in a number of 2N336 transistors with a wide range of Betas. Table V does not indicate any consistant correlation between the two parameters.

<u>Negative Bias Current on High Gain Transistor</u>

The split log-log plot of Figure 12 shows the results obtained in studying the effect of extending the biasing into the negative base current region. In high Beta transistors the gain held up quite well even with relatively large negative base currents and seemed to be well behaved with a very high peak of 150,000 with $I_b = -4 \times 10^{-11}$ amp. In lower Beta units ($\beta = 750$ at $I_b = +2 \times 10^{-10}$ amp, $V_{ce} = 1$ volt) the gain dropped much faster with negative base currents ($\beta = 0.5$ at $I_b = -2 \times 10^{-10}$ amp, $V_{ce} = 1$ volt).

Table IV. Data Taken on a High Gain 2N336 Transistor to Study the Effect of Reducing V_{cb}

V_{ce} mv	V_{be} mv	V_{cb} mv	I_{ceo} μamp	I_b amp	I_c μamp	Beta
1000	78	922	0.5	5×10^{-11}	1.4	19,000
				2×10^{-10}	3.4	10,000
83	60	23	0.17	5×10^{-11}	0.62	8,000
				2×10^{-10}	1.4	3,700
60	53	7	0.15	5×10^{-11}	0.48	6,000
				2×10^{-10}	1.05	2,500

Table V. Data Taken on Nine 2N336 Transistors that Shows no Correlation Between Beta and the Base-to-Emitter Voltage. ($I_b = 5 \times 10^{-10}$ amp, $V_{ce} = +0.5$ volt)

Beta	V_{be} mv	I_{ceo} amp
1	127.7	4×10^{-9}
3	94.7	5×10^{-10}
80	48.5	1.25×10^{-8}
750	21.0	6.8×10^{-8}
750	60.5	7.0×10^{-8}
750	58.1	7×10^{-8}
880	61.5	2.1×10^{-7}
1080	31.6	10^{-7}
4100	46.4	1.5×10^{-7}

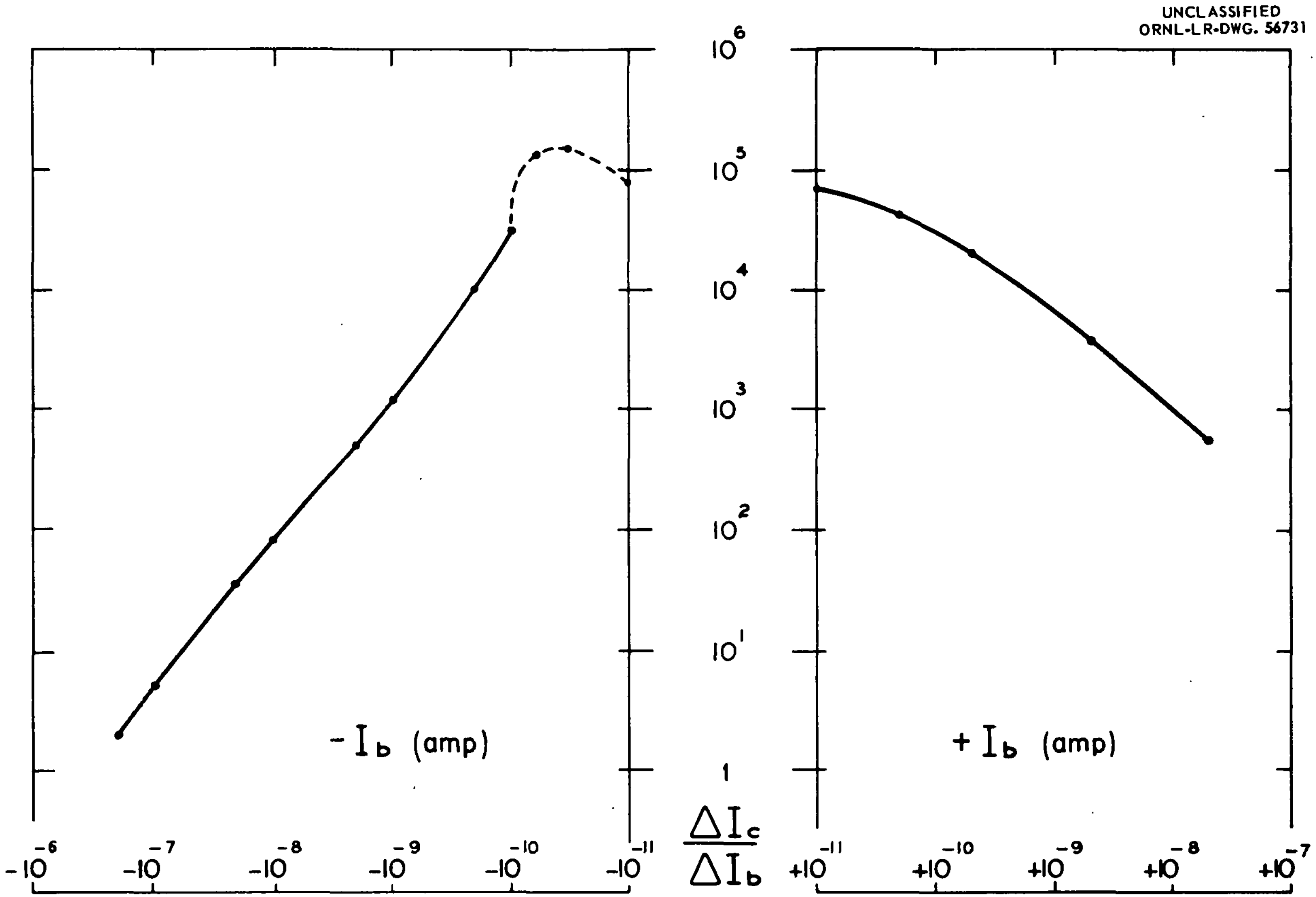

Fig. 12. Split Log-Log Plot Showing the Existence of a Large Beta Extending into the Region of Negative Base Currents in a High Gain Transistor. (V_{ce} = +1.0 volt)

POSSIBLE EXPLANATIONS OF HIGH GAIN EFFECT

Discussions with a number of people in the semiconductor development field have resulted in possible explanations that suggest the existence of a N type inversion layer on the P type base of the NPN silicon transistors of interest. It was suggested that perhaps in the assembly procedure the silicon bar was exposed to an environment of sufficient humidity to deposit a small amount of water on the base of some of the units. Water has the effect of inverting doped silicon from P to N type, hence the P type base could develop an N type inversion layer. (It should be noted that these transistors were finally sealed with a varnish or epoxy that was applied directly on the bar).

The process by which the current gain of such a transistor might increase probably involves the surface recombination action that has been a limiting factor in the design of modern transistors. The injected electrons from the emitter that are recombined by bulk recombination in the base and by surface recombination constitute the base current and obviously reduce the common base current gain α below unity.

$$\alpha = \frac{I_c}{I_e} = \frac{I_e - I_b}{I_e} = 1 - \frac{I_b}{I_e} \qquad (2)$$

Similarly the common emitter current gain, β, decreases.

$$\beta = \frac{I_c}{I_b} = \frac{I_e - I_b}{I_b} = \frac{I_e}{I_b} - 1 \qquad (3)$$

It is probably safe to assume[7] that surface recombination normally makes the largest contribution to I_b so that an appreciable reduction of that action would allow α to approach unity and β to approach a very large value.

Two simplified models might have caused a desirable recombination reduction. One model would rely on an electric field effect that would be set up from the N inversion layer in a manner that would repel most of the normally recombined injected electrons away from the surface allowing them to continue a more directional diffusion through the base region to the collector. Such a model, of course, would require properly assumed respective potentials in the various regions of the transistor. For example, the N inversion layer would have to be at least slightly negative with respect to the base so it would have to derive a potential from the emitter region. A second model would picture the N inversion layer as an extension of the collector forming a very efficient collection geometry that would surround the base and very conveniently "intercept" most injected electrons that would normally be recombined at the surface.

Both of these models can be made consistent in terms of two very clear experimental observations. First, the existence of a N inversion layer would most likely allow the "leakage" current, I_{ceo}, to increase since there would be a relatively low resistance "channel" from emitter to collector. Figures 4 and 5 show that I_{ceo} was highest in the units with high current gain. Second, the decrease in current gain with increasing current levels could be explained in terms of the current densities in the base region.

In the electric field model the ability to repel the electrons away from the surface could be overcome as the current density increased forcing the electrons flowing in the base toward the surface. In the extended collector model an increased current density would require that more current flow in the thin N inversion layer. The ability of this layer to efficiently carry the "intercepted" electrons to the real collector could involve a current saturation which would effectively reduce the high gain effect with increasing current by "exposing" the surface recombination centers that would also exist on the N inversion layer.

Two more facts point toward the possibility of the effect being caused by a water induced inversion layer. First, the manufacturing procedure employed by Texas Instruments in producing the 2N336 and 2N338 units was changed in August of 1960 and the effect seems to have been altered. This change in part was made to reduce the possibility of the transistors being exposed to moisture during the assembling. Second, by very crude techniques a General Electric 2N338 with a Beta less than one for I_b less than 10^{-7} amp was opened and exposed to steam, then the bar was coated with an epoxy. A temporary increase in the low current Beta was observed as noted in Table VI. The increased Beta lasted for a few days.

A research and development program has been started by a commercial semiconductor manufacturer with the expressed purpose of trying to reliably produce transistors with N inversion layers that have characteristics comparable to those described in the previous sections. This work should prove very helpful in arriving at a more exact description of the effect of the N inversion layer.

Table VI. Beta Test of a General Electric 2N338 Transistor that was Opened and Exposed to Steam for 10 Minutes. Originally the Transistor had a Beta Less than One for all Currents Below 10^{-7} amp (V_{ce} = +1.0 volt)

I_b	I_c	Beta
0	3.7×10^{-7}	
5×10^{-11}	3.8×10^{-7}	150
5×10^{-10}	4.5×10^{-7}	50
5×10^{-9}	6.1×10^{-7}	10
10^{-8}	6.8×10^{-7}	6.5
5×10^{-8}	9.3×10^{-7}	2.7
10^{-7}	1.1×10^{-6}	2.2
5×10^{-7}	2.1×10^{-6}	2
10^{-6}	3.4×10^{-6}	2.5
5×10^{-6}	1.7×10^{-6}	6.4

CURRENT AMPLIFIER CIRCUIT ANALYSIS

Before describing the utilization of a high gain transistor in a current amplifier circuit, it is in order to first discuss the analysis of current amplifiers so that an applicable criteria can be set up for the amplifier design. For direct current measurements that do not employ chopping techniques there are three basic ways of using an amplifier. These are with no feedback, with shunt feedback, and with series feedback.

VACUUM TUBE AMPLIFIER ANALYSIS

The usual analysis[8] of the three gives the results shown in Figures 13, 14, and 15. The symbols used are as follows:

- I = Input current from detector considered to be a source with infinite resistance.[3]
- C_d = Detector capacitance and the capacitance to ground of the input circuit wiring.
- R_1 = Detector load resistance in parallel with leakage resistance to ground.
- C_1 = Shunt capacitance of R_1
- R_p = Input resistance of electrometer.
- C_p = Input capacitance of electrometer.
- R_f = Feedback resistance
- C_f = Shunt capacitance of R_f
- A = Amplifier open loop voltage gain possessing dynamics that do not enter into the response characteristics since they are much faster than those imposed by feedback and input impedances.
- T_r = $\frac{1}{e}$ response time to a current step input. With the mentioned dynamics of A this is simply the time constant of a first order lag.
- e_o = Output voltage

UNCLASSIFIED
ORNL-LR-DWG. 56732

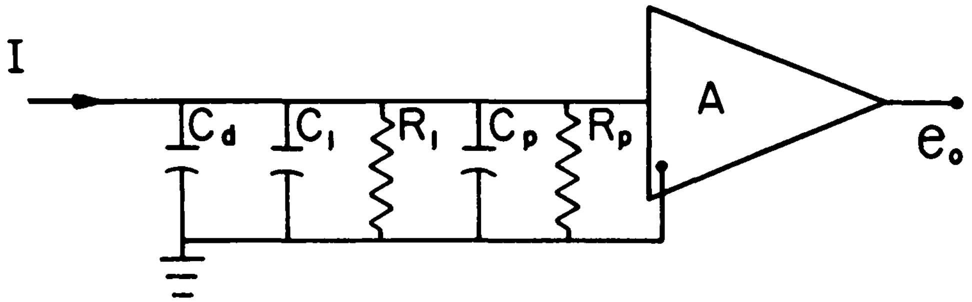

$$e_o = A\,I\,\frac{R_1 \cdot R_p}{R_1 + R_p}\left(1 - \exp\left(-\frac{t}{T_r}\right)\right) \cong A\,I\,R_1\left(1 - \exp\left(-\frac{t}{T_r}\right)\right) \qquad (4)$$

$$T_r = \frac{R_1\,R_p}{R_1 + R_p}\left(C_d + C_1 + C_p\right) \cong R_1\left(C_d + C_1 + C_p\right) \qquad (5)$$

Approximation $R_p \gg R_1$

Fig. 13. Transfer Equations of an Unfedback Current Amplifier from an Analysis Using a Forward Loop Voltage Gain (A) That Operates on Voltage Developed at the Input

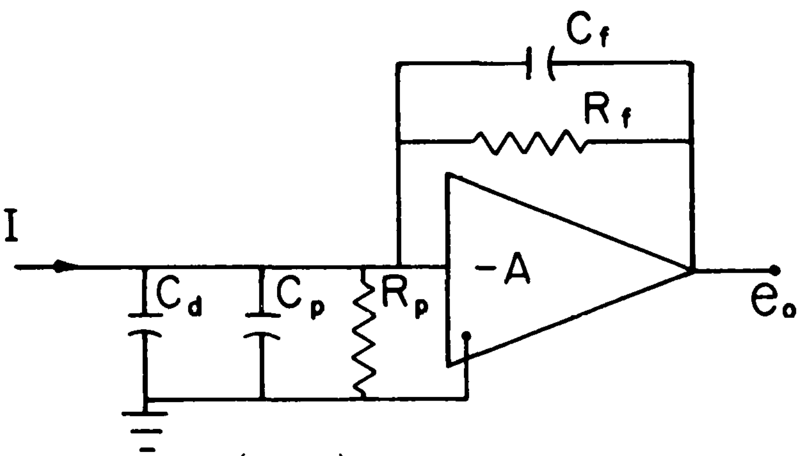

$$-e_o = \frac{A}{A+1} \cdot \frac{I\,R_f(A+1)\,R_p}{R_f + (A+1)\,R_p}\left(1 - \exp\left(-\frac{t}{T_r}\right)\right) \cong I R_f\left(1 - \exp\left(-\frac{t}{T_r}\right)\right) \qquad (6)$$

$$T_r = \frac{R_f(A+1)\,R_p}{R_f + (A+1)R_p}\left(C_f + \frac{C_p + C_d}{A+1}\right) \cong R_f\left(C_f + \frac{C_p + C_d}{A+1}\right) \qquad (7)$$

Approximations $(A + 1)\,R_p \gg R_f \qquad A \gg 1$ (8)

Fig. 14. Transfer Equations of a Shunt Fedback Current Amplifier from an Analysis Using a Forward Loop Voltage Gain (-A) That Operates on Voltage Developed at the Input

UNCLASSIFIED
ORNL-LR-DWG. 56733

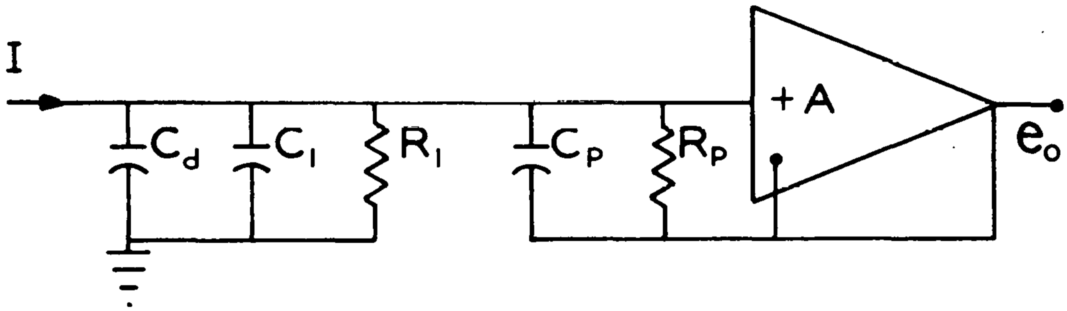

$$e_o = \frac{A}{A+1} \quad \frac{I\,R_1\,(A+1)\,R_p}{R_1 + (A+1)\,R_p} \quad (1 - \exp(-\frac{t}{T_r})) \cong I\,R_1(1-\exp(-\frac{t}{T_r})) \qquad (9)$$

$$T_r = \frac{R_1(A+1)\,R_p}{R_1 + (A+1)\,R_p} \quad (C_d + C_1 + \frac{C_p}{A+1}) \cong R_1\,(C_d + C_1 + \frac{C_p}{A+1}) \qquad (10)$$

Approximations $(A + 1)\,R_p \gg R_1 \qquad A \gg 1$ (11)

Fig. 15. Transfer Equations of a Series Fedback Current Amplifier from an Analysis Using a Forward Loop Voltage Gain (A) That Operates on Voltage Developed at the Input

Another term that applies in a more complete analysis is an equivalent voltage source (offset voltage) appearing in series with the input tube as a result of cathode temperature variations or contact potential variations. These variations arise from supply voltage drifts and/or aging effects in the tube.

The unfedback circuit is quite popular in many electrometer applications where the d-c drift is small and the input resistance is sufficiently large to allow for large detector resistors. The shunt fedback circuit (so named because the current through the feedback path is shunted across the amplifier and summed at the input with the detector current) is the configuration commonly used for making current measurements. However, the series fedback circuit (so named because the fedback voltage is applied in series with the incoming signal) is also useful and has the desirable characteristic of not requiring a direct connection between the feedback resistor and the signal source.

TRANSISTOR AMPLIFIER ANALYSIS

To speak of a voltage gain when employing transistors is somewhat different than the well known voltage gain terminology employed in the vacuum tube analysis. The fact that the actual gain in transistors is due to their current amplification properties points out a possible need for an analysis of transistor amplifiers in terms of current gain instead of voltage gain (somewhat analogous to an approach by Shea[9]). To speak of voltages one needs to know only a current gain and some transfer resistance to change to a voltage output.

With this in mind, an analysis of the previously treated circuit configurations follows in Figures 16, 17, and 18.

In this analysis the previously defined symbols, when used, apply. Also, the dynamics of the forward loop except for the input are again considered to be much faster than the other time constants of the system so that they can be neglected. The difference in the voltage gain and current gain approaches is expressed by β, which represents the forward open loop current gain up to the output circuit, and R_T which is the transfer resistance of the output circuit. The current that β operates on is i which flows through the input resistance R_p. This then says that for a current, i, flowing through R_p there exists a current βi flowing into the output circuit, resulting in an output voltage of

$$e_o = \beta i R_T. \tag{20}$$

The equations describing the unfedback amplifier give results that are similar to those using the usual voltage gain approach. This can be easily seen by noting that for an input current i the input voltage is iR_p and the output voltage is $\beta i R_T$ so that the voltage gain is, by definition,

$$A = \frac{e_o}{e_{in}} = \frac{\beta i R_T}{i R_p} = \frac{\beta R_T}{R_p} \tag{21}$$

UNCLASSIFIED
ORNL-LR-DWG. 56734

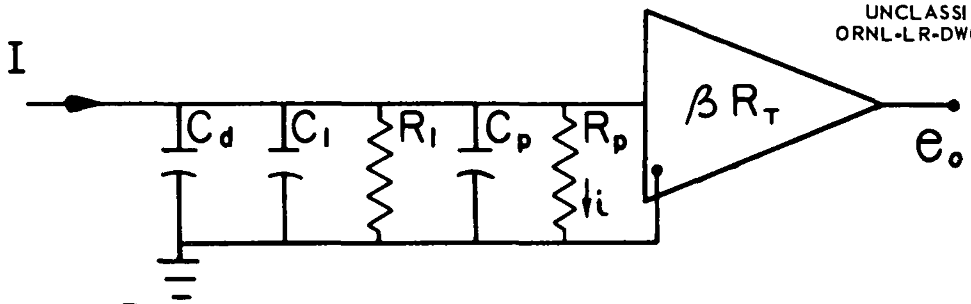

$$e_o = I\beta R_T \frac{R_1}{R_1 + R_p} (1 - \exp(- \frac{t}{T_r}) \cong I R_1 \frac{\beta R_T}{R_p} \tag{12}$$

$$T_r = \frac{R_1 R_p}{R_1 + R_p} (C_d + C_1 + C_p) \cong R_1 (C_d + C_1 + C_p) \tag{13}$$

Approximation $R_p \gg R_1$

Fig. 16. Transfer Equations of an Unfedback Current Amplifier from an Analysis Using a Forward Loop Transfer With the Dimension of Resistance That Operates on the Current That Flows in the Input Resistance, R_p

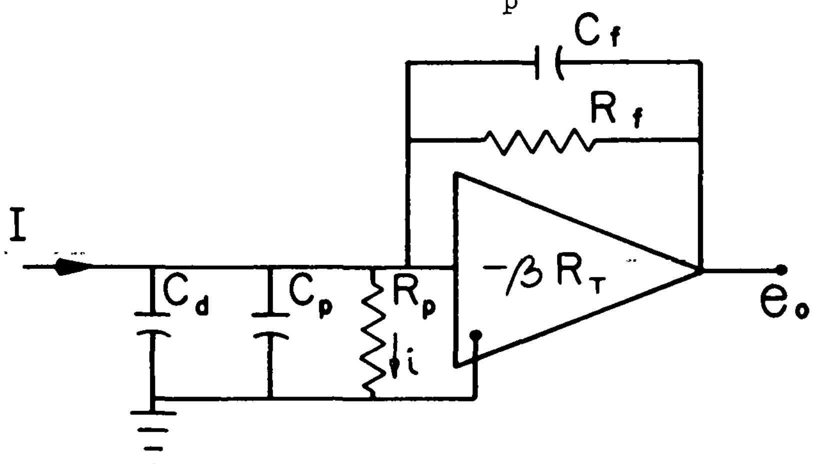

$$-e_o = IR_f \frac{\beta R_T}{R_f + R_p + \beta R_T} (1 - \exp(- \frac{t}{T_r})) \cong IR_f(1 - \exp(- \frac{t}{T_r})) \tag{14}$$

$$T_r = \frac{R_f(R_p + \beta R_T)}{R_f + R_p + \beta R_T} \left(\frac{C_p + C_d}{1 + \frac{\beta R_T}{R_p}} + C_f \right) \cong R_f(C_f + \frac{R_p}{\beta R_T}(C_p + C_d)) \tag{15}$$

Approximation $\beta R_T \gg R_f + R_p$ (16)

Fig. 17. Transfer Equations of a Shunt Fedback Current Amplifier from an Analysis Using a Forward Loop Transfer With the Dimensions of Resistance that Operates on the Current That Flows in the Input Resistance, R_p

UNCLASSIFIED
ORNL-LR-DWG. 56735

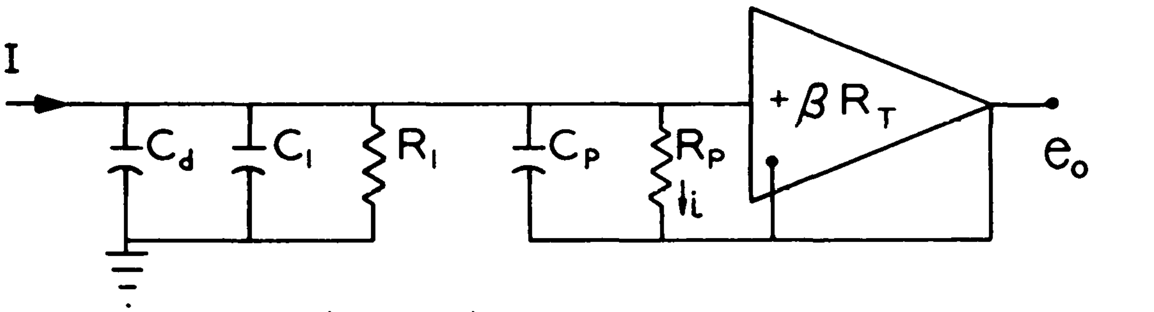

$$e_o = \frac{1}{1 + \frac{R_p}{\beta R_T}} \quad \frac{I\,R_1(\beta R_T + R_p)}{R_1 + R_p + \beta R_T} \left(1 - \exp\left(- \frac{t}{T_r}\right)\right) \cong I\,R_1\left(1 - \exp\left(-\frac{t}{T_r}\right)\right) \qquad (17)$$

$$T_r = \frac{R_1(R_p + \beta R_T)}{R_1 + R_p + \beta R_T} \left(C_d + C_1 + \frac{C_p}{\frac{\beta R_T}{R_p} + 1}\right) \cong R_1 \left(C_d + C_1 + \frac{R_p}{\beta R_T} C_p\right) \qquad (18)$$

Approximation $\beta R_T \gg R_1 + R_p$ (19)

Fig. 18. Transfer Equations of a Series Fedback Current Amplifier from an Analysis Using a Forward Loop Transfer With the Dimension of Resistance That Operates on the Current That Flows in the Input Resistance, R_p

Substituting in this value for A in equation 4 gives again equation 12. The form of equation 12, however, points out more clearly the effect of very high input resistance on the total transfer from an input current to an output voltage. More clearly, from equation 21, the fact that the voltage gain becomes small as R_p increases reveals the true input current characteristics of a transistor amplifier that have to be considered as opposed, for example, to electrometer tubes that can operate at absolutely minimum grid currents (less than 10^{-14} amp) to keep their input resistance at a maximum and still maintain reasonable voltage gain. The obvious requirement for maintaining a voltage gain is to make the condition $\beta R_T \gg R_p$ exist in the transistor amplifiers. The direct substitution of $\frac{\beta R_T}{R_p}$ for A in all three cases makes the desired transformation from voltage gain to current gain.

A quick look at the conditions necessary for the use of an unfedback configuration reveals some undesirable conditions that made it impractical. Primarily these were the usual drawbacks of such transistor amplifiers in terms of non-linearity, input resistance requirements, d-c drift, and a-c noise.

The series and shunt fedback arrangements impose important requirements upon the value of βR_T in that this total transfer resistance must be much greater than R_p plus R_f (or R_1). The fact that series feedback fails to degenerate the capacitance $C_d + C_1$ immediately demands a reduction in R_1, if the major time constant, T_r, is to be reduced, for in general $C_d + C_1$ will be much larger than $(R_p/\beta R_T)\ C_p$ so that it would become the major capacitance in this configuration. The degenerated capacitance $(R_p/\beta R_T)\ C_p$ in the best amplifiers has been experimentally shown to be small compared to $0.4\ \mu\mu f$, (Appendix IX). Although this configuration does offer some interesting possibilities in particular applications (for example it has very high input resistance) it was not used in the amplifiers to be described.

THE CHOICE OF SHUNT FEEDBACK

In the shunt fedback case, upon fulfillment of the criterion $\beta R_T \gg (R_f + R_p)$, the accuracy of the d-c gain of the amplifier is a function only of the fedback resistor R_f. The practical limitation is the equivalent d-c current drift at the input to the amplifier which cannot be distinguished from signal current. This equivalent current results mainly from the temperature effect on I_{cb} of the input transistor. The analysis does not show the summing of the shunt current at the output junction, but this effect can be easily shown to be negligable by the factor of $R_o/\beta R_T$ where R_o is the output resistance of the forward loop amplifier. As possible numbers of interest the value of βR_T, from experiments on the amplifiers, is as large as 2×10^{13} ohms and $R_o = 1.8 \times 10^3$ ohms. The most obvious significance of these numbers is derived from βR_T which suggests the use of feedback resistors of the order of 10^{11} ohms with reasonable accuracy on the d-c gain.

Since shunt feedback was employed in the amplifiers to be described, the output resistance, R_o', of the closed loop is significant in terms of the total transformation of resistance level that goes from an essentially infinite resistance at the detector to a low valued R_o' capable of driving most any recording device desired. The derivation of R_o' by a half-amplitude method (Appendix III) shows this value to be

$$R_o' \cong \frac{R_o}{\beta R_T/(R_f + R_p)}. \tag{42}$$

The open loop output resistance is obviously reduced by the factor $\frac{\beta R_T}{R_f + R_p}$ which, because of its importance in determining the fedback circuit characteristics, might be referred to as the feedback factor. Some measurements of R_o' are presented in a later section.

The shunt fedback analysis applies to all of the following circuit design. This configuration was chosen for its desirable characteristics of linearity and stable operation with relatively simple zero and sensitivity control. Also, the degeneration of C_p and C_d by the factor $(R_p/\beta R_T)$ makes C_f a predominant capacitance of the circuit so that added a-c noise level improvement was available at the expense of response time by increasing C_f with a small fixed capacitance. Experiments described in later sections bring out these points more clearly.

Some terminology used in describing the amplifiers and their characteristics includes the sensitivity, expressed as the current I necessary for an output voltage of 1 volt, which from equation 14 is simply

$$\text{sensitivity} = \frac{e_o}{I} = R_f \quad . \tag{22}$$

Also, all noise and drifts will be referred to the input as equivalent currents, although they were actually measured by noting the output voltage, by the same equation

$$I = e_o/R_f . \tag{23}$$

The references to response or risetime involve equation 15.

"α AMPLIFIER" DESIGN

Based upon the described transistor characteristics and shunt fedback analysis, amplifiers have been designed to study the actual behavior of the transistors when utilized in the input stages. One of the amplifiers, Figure 19, is of particular interest since it utilizes those transistors found to possess the largest current gain characteristics. This amplifier is referred to as the "α amplifier" to simplify references in the following discussion of its characteristics. Four such amplifiers have been built for tests and applications.

INPUT CIRCUIT

The first and most significant consideration in the design was the manner in which the input transistor, Q_1, was selected and incorporated into the circuit shown in Figure 20. Utilizing the transistor tester of Figure 3 the first criterion was that the current gain, with $I_b = 5 \times 10^{-11}$ amp, $V_{ce} = 1$ volt, be greater than 10,000. Also the "leakage" collector current, I_{ceo}, was noted for biasing conditions that followed the first transistor. The current level at which this transistor operated was certainly well below that considered "normal" in conventional design since the collector current was adjusted to approach the value of I_{ceo} by biasing the output voltage to approximately zero potential with respect to ground. (Note that there was no fixed positive bias current into the base of Q_1). This then says that under these

UNCLASSIFIED
ORNL-LR-DWG. 56736

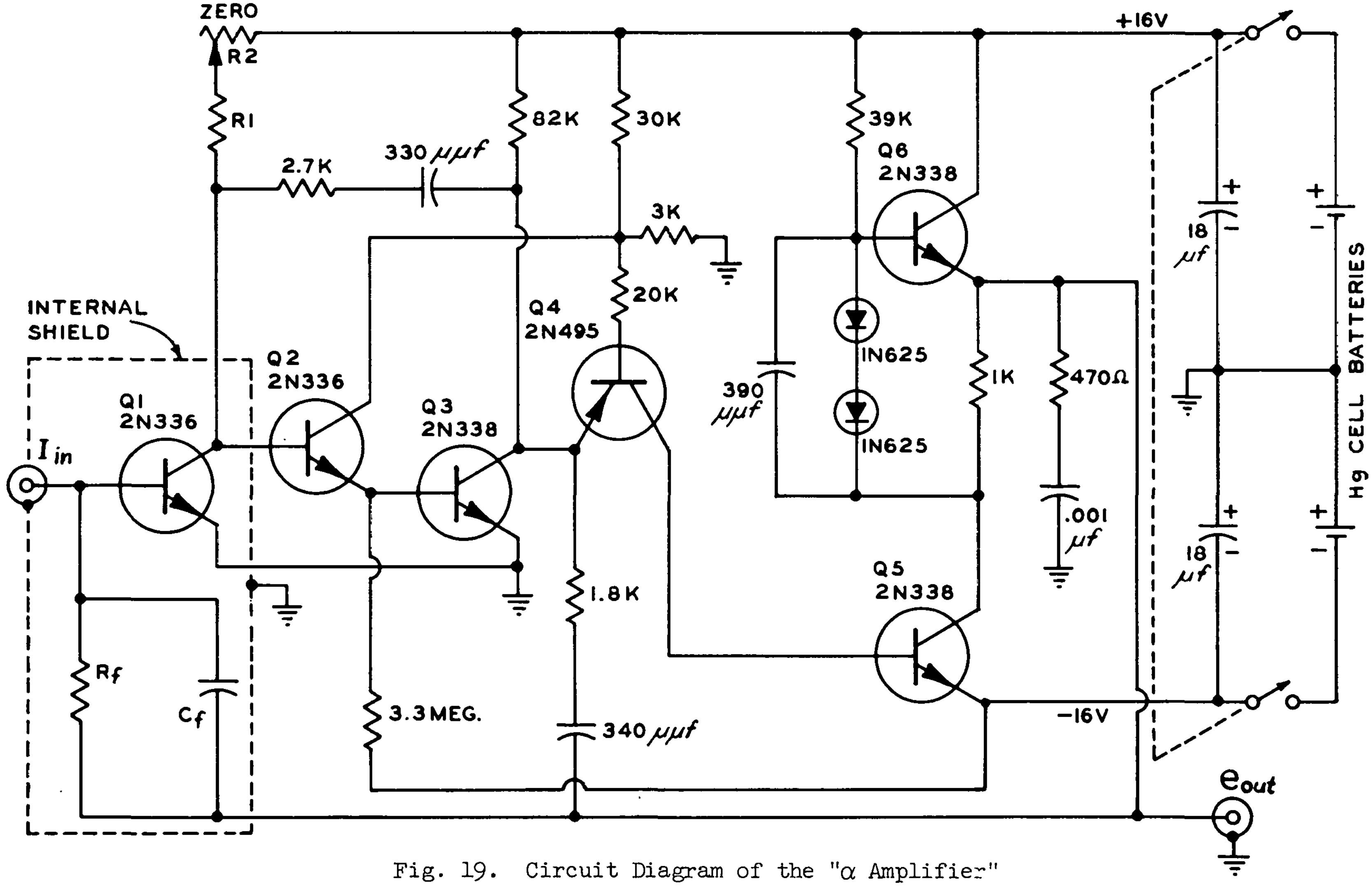

Fig. 19. Circuit Diagram of the "α Amplifier"

conditions the actual feedback current through R_f into the input base was essentially reduced to zero so that only the "leakage" collector current was allowed to flow in Q_1. The desirability of this mode of operation was obvious from the behavior of the high gain characteristics at very low base current, Figure 5. The rapid increase in current gain with decreasing base current suggested the highest realization of these unusual characteristics when the base current was at an absolute minimum. This base current under "zero" conditions was simply $i_{b_1} = \dfrac{e_o - V_{be1}}{R_f}$.

Since V_{be}, from the data of Tables IV and V, under the zero and low base current conditions was in the order of +50 to +100 millivolts any near zero output level sufficiently reduced i_b to approach this optimum condition.

Q_1 was connected in the common emitter configuration to take advantage of maximum power gain so that a minimum of circuitry was needed to get the signal level into a more normal level of operation.

Due to the high impedance and extra-sensitive level of operation of the feedback resistor and input transistor, they were carefully mounted in a shielded box inside of the regular amplifier box for proper noise considerations. The usual insulation and lead shielding problems involved at such high impedance levels were carefully taken care of to minimize them as sources of leakage and noise.

UNCLASSIFIED
ORNL-LR-DWG. 56737

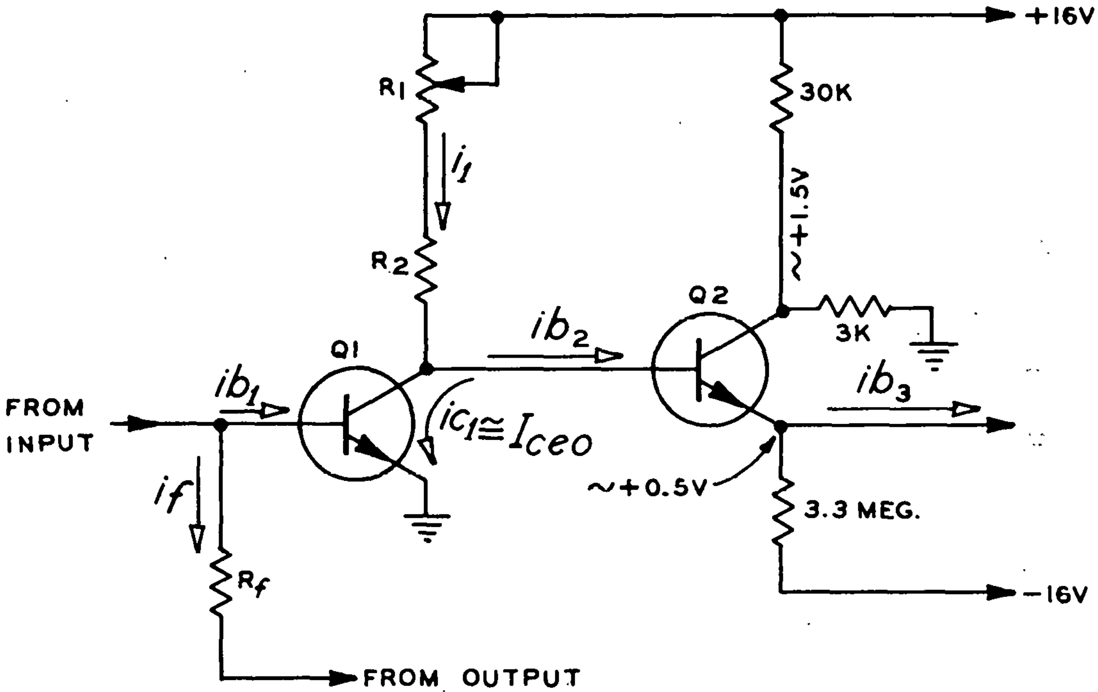

Fig. 20. Input Circuit of "α Amplifier"

BIASING

The biasing referred to in the previous discussion was controlled by varying the load resistor of Q_1. The value of this load ($R_1 + R_2$) was chosen by allowing the total load current to be only slightly greater than that necessary to supply the "leakage" collector current of Q_1. This current, due to its low value, was derived from a relatively large resistance and was made fairly constant by using a positive voltage supply of +16 volts so that any normal variation of the base voltage of Q_2 appeared as a second order effect. Since the voltage of the base of Q_2 with respect to ground was approximately 1 volt the load resistor of Q_1 was

$$R_1 + R_2 \cong \frac{15}{I_{ceo_1} + I_{b2}} \quad \text{ohms}. \tag{24}$$

The selection of Q_2 also involved the use of the special transistor tester with the criterion being a current gain of approximately 100 with $i_{b2} \cong 10^{-7}$ amp. Such a gain at this level insured sufficient current gain from the emitter-follower application of Q_2 so that Q_3 could operate at a "normal" collector current (approximately 170 microamps). Q_3 was not a special transistor since it operated at a "normal" current level so it could be arbitrarily picked from any suitable NPN silicon type.

DIRECT CURRENT COUPLING

The manner in which Q_4 was used, Figure 21, was chosen mainly to provide a method of d-c coupling from the collector of Q_3, which was positive with respect to grcund, to the base of Q_5, which was negative with respect to ground. There were a number of other ways of accomplishing coupling that provides for an output with a dynamic ± voltage range, but this seemed to be the best in terms of necessary voltage supplies and noise. This application obviously utilized the PNP voltage characteristics of Q_4 in that the difference in d-c level appeared from collector to emitter in the common-base connection. Also, due to the base-to-emitter voltage necessary for the operation of Q_4, the collector-to-emitter voltage of Q_3 was determined by the choice of the base-to-ground voltage of Q_4 which, of course, was derived from the resistor string from +16 volts to ground. A minor sacrifice resulting from this coupling came from the common-base current gain, α_4, of Q_4 which was slightly less than one. Q_4 was a PNP, silicon, surface barrier, transistor manufactured by Philco and it was found that at the collector current (approximately 15 microamps) at which it operated most transistors of this type had an $\alpha \cong .90$. Also, interpolating from the manufacturers' specifications, the common base input resistance was of the order of 1 kilohm and the output resistance was approximately 1 megohm. This provided an adequate continuation of the idea of thinking in terms of the current gain in the stages preceding the output circuit since the resistance levels of Q_4 could easily drive the current, $i_{b5} = \beta i_{b1}$, into the base of Q_5.

UNCLASSIFIED
ORNL-LR-DWG. 56738

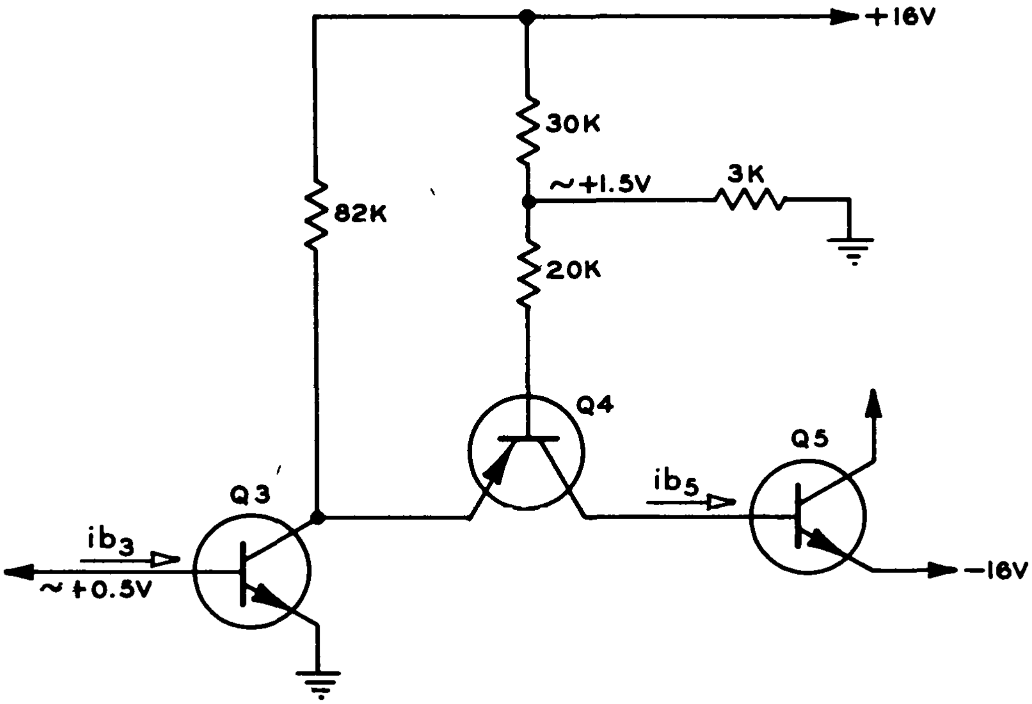

Fig. 21. Direct Coupling of "α Amplifier" Allowing for an Output with a Dynamic ± Voltage Range

OUTPUT CIRCUIT

The output circuit, Figure 22, had some interesting characteristics that proved to be quite useful for this type of amplifier. The manner in which the transistors Q_5 and Q_6 were used might at first be thought of as being analogous to the dynamic plate follower[10] which has been used in various vacuum tube applications. However, it was somewhat different, again due to the difference in current and voltage devices. Even so, a proper descriptive name for the circuit might be a "dynamic collector follower" since Q_6 was an active element in the collector circuit of Q_5.

This circuit essentially established the output characteristics of the open loop amplifier so that it was desirable to know its output resistance R_o and its transfer resistance R_T. The emphasis upon R_o was obvious since the output must be at a resistance level capable of driving read out instruments such as recorders, voltmeters, and oscilloscopes. This value was improved by feedback as shown in Appendix III. The need for a large value of R_T followed from the amplifier analysis which used R_T in the description of the forward loop characteristics. To clarify its definition, R_T was equal to the ratio of the output voltage to the current into the output circuit which, in this case, was the base current of Q_5. Therefore

$$R_T = \frac{e_o}{i_{b5}} \quad . \tag{25}$$

UNCLASSIFIED
ORNL-LR-DWG. 56739

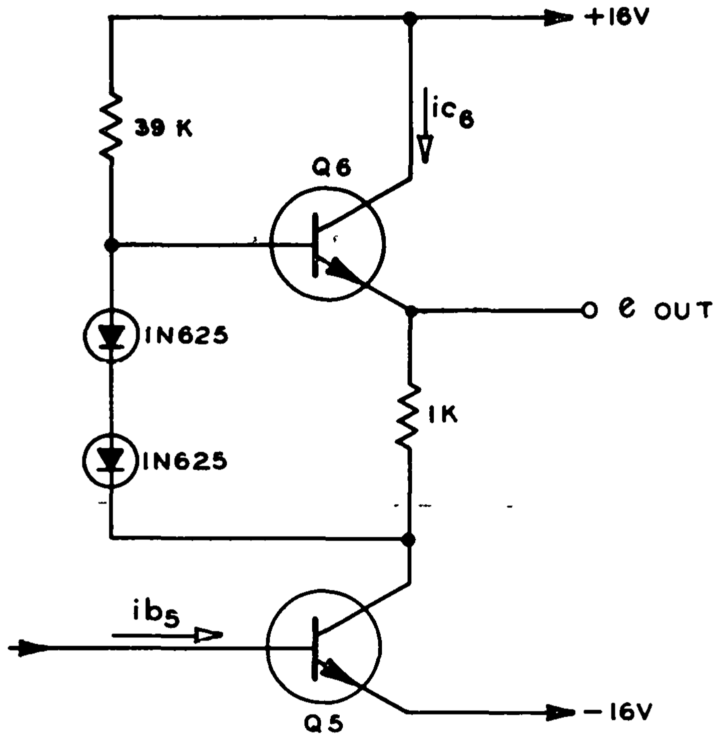

Fig. 22. Output Circuit of "α Amplifier"

An approximate analysis of the output circuit (Appendix IV) suggested that to a first approximation

$$R_o \cong \frac{R \quad R_6}{\beta_{5,6} \ r} \cong \frac{R \, R_6 \quad I_{c6}}{\beta_{5,6} \ e'} \qquad (55), (58)$$

and that

$$R_T \cong \beta_{5,6} \quad R \qquad (59)$$

The actual behavior of the circuit was studied experimentally by the use of the test circuit of Figure 23. The condition set by the driving resistance of 100 K Ω was assumed to be sufficient to be considered as a current source to approximate the conditions of the amplifier circuit. The input resistance of Q_5, with a collector current of approximately one milliampere, was approximately 6 K Ω as taken from the curve of Figure 31. Also R_6, input resistance of Q_6, came from the same curve. Some sample data are shown in Table VII.

The interdependence of the parameters followed the derived equations to the extent that an increase or decrease of R_o or R_T could be predicted. All of the values of R_o measured were grouped in a reasonable range that was acceptable for the amplifier. The term of most significance, however, was R_T which was to be maximized to achieve maximum benefits from the forward gain characteristics of the amplifier as emphasized throughout the amplifier analysis. The values chosen for the final design were

$R = 39$ KΩ $\qquad$ $r = 1$ KΩ

$e' = .7$ volt (derived with 2 silicon diodes)

This yielded the resistances

$$R_o = 1.8 \times 10^3 \ \Omega$$

$$R_T = 2 \times 10^6 \ \Omega$$

The collector resistance of Q_5 and the d-c operating conditions set the practical limits on R_T.

A brief look at the significance of these values revealed an obvious advantage of this output circuit over a standard circuit such as the one of Figure 24. The analogous values from a simple analysis are

$$R_o = R_L = 1.8 \times 10^3 \, \Omega$$

$$R_T = \beta_{5,6} \times 1800 = 1.4 \times 10^5 \ \Omega$$

with a d-c collector current of approximately 9 milliamperes. If an increase in R_o were acceptable, R_T could be increased to approach the analogous value of the dynamic collector follower. These resistances would be

$$R_T \cong 2 \times 10^6 \ \Omega$$

$$R_o = R_L = 20 \times 10^3 \, \Omega$$

with a d-c collector current of 800 μa.

The dynamic collector follower combines the most acceptable combination of low R_o and high R_T by an order of magnitude over a standard common-emitter stage.

COMPENSATION AGAINST OSCILLATIONS

Upon the completion of the design of the forward loop of the amplifier with all due consideration given to the attainment of optimum conditions of input impedance, current gain, d-c coupling, biasing, transfer resistance and output resistance, there still existed an important problem that required attention before shunt feedback could be successfully employed. This was the suppression of all oscillations that could occur when certain feedback impedances were tested. The feedback components tested were resistors ranging from 10^3 to 10^{12} ohms and a 0.01 μf capacitor.

The main compensation was derived from the series R-C networks from the output to the collector of Q_3 and from the collector of Q_3 to the collector of Q_1. By virtue of this type of interstage feedback a reasonable degree of gain and phase margin could be realized. There was quite a bit of difficulty encountered in attempting to calculate necessary values for these R-C networks because of complicated equivalent transistor circuits coupled with an uncertainty of the values that even approximately fit the equivalent circuits. The actual selection of the networks, therefore, was made experimentally based upon previous experience. (The amplifier of Figure 2, for example, was corrected against oscillation by the same techniques). Feedback similar to this has been used[11] for neutralization in the design of wide bandwidth amplifiers.

When using the lowest values of feedback resistance, small trimming capacitors were necessary to control the current step response characteristics. Care had to be taken in the final selection of the added capacitance to prevent oscillations or underdamped ringing. The trimming capacitors also served to decrease the a-c noise level, with the usual sacrifice of rise-time, as pointed out in a later section.

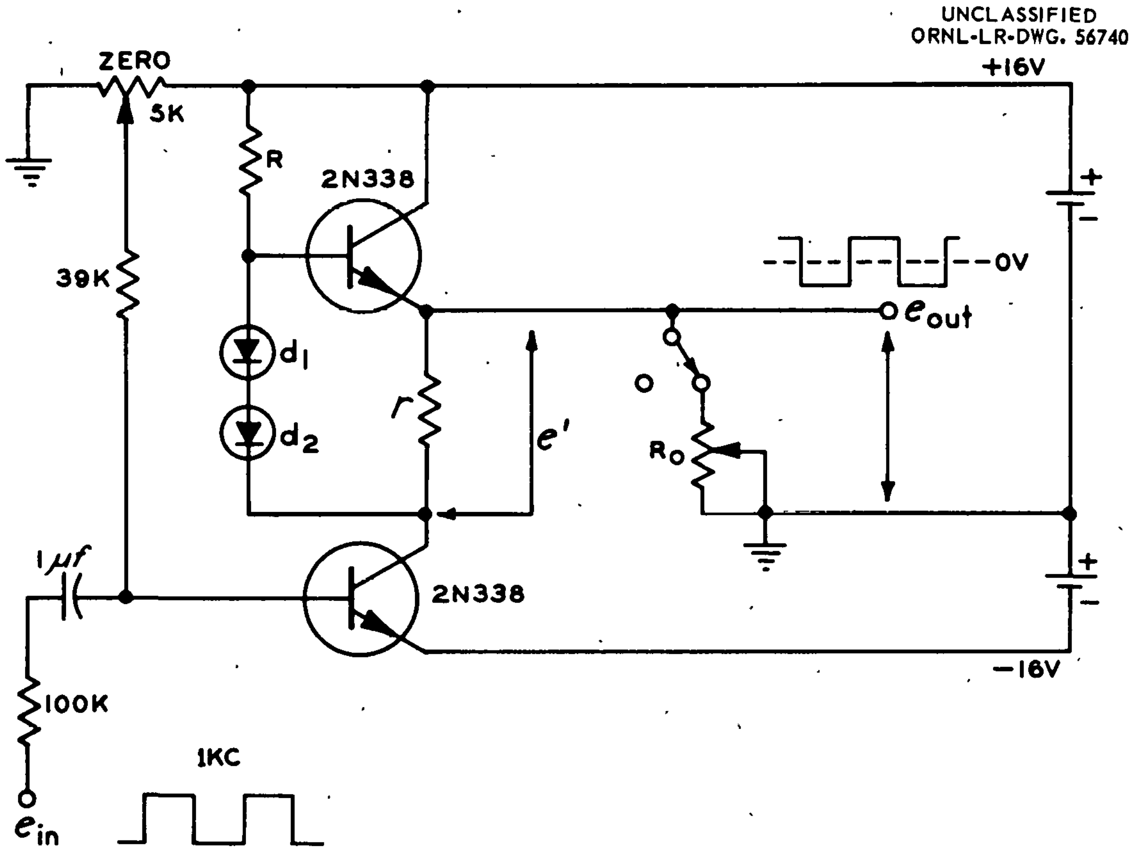

Fig. 23. Arrangement for Testing the Transfer Resistance, R_T, and the Output Resistance, R_o, of the Output Circuit

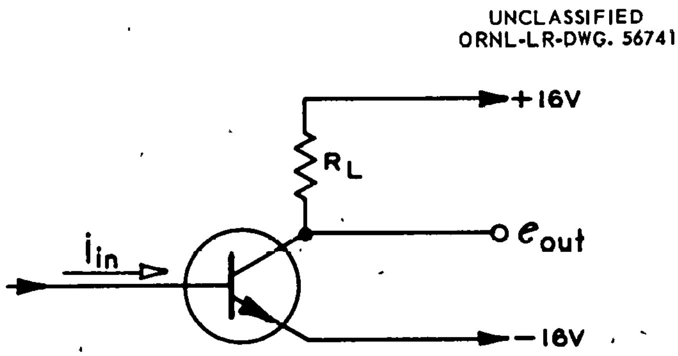

Fig. 24. A Simple Output Circuit

Table VII. Experimental Data Taken on the Output Circuit to Note the Effect of Circuit Parameters on R_o and R_T

R Kilohms	r Ohms	d_1 diode type	d_2 diode type	R_o Kilohms	R_T Megohms
39	1000	Si	Si	1.8	2.0
39	470	Si	Si	1.35	1.7
39	220	Si	Si	0.84	1.2
68	220	Si	Si	1.2	1.6
68*	1000*	Si	Si	2.2	3.0
100*	1000*	Si	Si	2.8	3.6
39	235	Si	Ge	1.1	1.2
39	470	Si	Ge	2.4	1.36
68	235	Si	Ge	3.8	1.6
68	470	Si	Ge	5.2	2.0

*These conditions limited the output dynamic range

EXPERIMENTAL METHODS FOR THE STUDY OF AMPLIFIER CHARACTERISTICS

The results of equation 14 plainly showed that when the necessary conditions of the forward gain were met, the input signal, in the form of a current, was reflected at the amplifier output, in the form of a voltage, with the transfer element being R_f. Therefore, R_f controlled the amplifier sensitivity permitting a very useful series of experiments to study the behavior of the "α amplifier".

The previously mentioned oscillation suppression allowed for an extremely wide range of feedback resistors adding to the possibilities of the ultimate utility of the amplifier. The experimental data presents the amplifier characteristics in a form that allowed for a true evaluation of the entire range of operation. Of prime importance was a knowledge of the ultimate limits of useful operation in the region of input currents extending down to the micro-microampere level. Operation in and above the microampere level was studied only briefly as a matter of record since there was no difficulty in designing simpler amplifiers for that region.

The major characteristics that were noted included:

1. Ability to yield accurate, linear sensitivity in the transfer from input current to output voltage
2. Response time

provided a measurement of the input base time constant R_pC_p in addition to information on open loop response and βR_T.

A-C NOISE

Within the bandwidth of the amplifier there existed an appreciable amount of inherent a-c noise. This noise was most easily reduced by the addition of a small amount of feedback capacitance. This, of course, was accomplished with an associated sacrifice in response time since any feedback capacity changed the time constant of equation 15. For this reason it should be understood that, since slight changes in the equivalent noise-bandwidth characteristics for any feedback resistance of interest could be made by the choice of the feedback capacitance, the associated values of R_fC_f were mainly chosen for satisfactory demonstration purposes and could be varied slightly. The main exceptions occurred in the examples of feedback resistance below 10^8 ohms. At those resistance levels there were undesirable positive feedback conditions resulting in oscillations of the order of a megacycle if the feedback capacitance was not large enough.

A simple experiment to get a feeling for the frequency composition making up the total a-c noise utilized series R-C output circuits as shown in Figure 25 with pictures of traces. This, of course, only gave the attenuation of noise amplitude that resulted from the low pass filter action.

oscilloscope readings. The square wave method was the only one used to study the sensitivity for feedback resistors greater than 10^{10} ohms because of excessive d-c drift at those sensitivity levels.

RESPONSE TIME

Measurements of the fedback amplifier response time over the entire range of sensitivities were also made by the square wave method of Appendix VI. To insure a reliable response one precaution that had to be made was to be sure that the time constant of the driving resistor with its intrinsic shunt capacity was much less than the time constant $(R_f C_f)$ of the fedback impedance. Failure to fulfill this condition resulted in a significant derivative term that would distort the true current response time.

A second method of determining the basic response time of the amplifier followed from the pulse technique described in Appendix VII. This served as a good check on the first method and also gave an indication of the forward loop response time.

The pulse method allowed the very interesting measurement of the unfedback amplifier characteristics allowing an experiment involving no d-c current into the input base so that actual "floating base" characteristics could be studied in an amplifier circuit. This condition of essentially infinite feedback impedance

3. a-c noise
4. d-c drift at ambient temperature and with temperature variation
5. Output resistance

The methods employed to study the above are described so that a fair evaluation of their true significance can be made. Whenever possible, different methods of determining certain characteristics were used as a check of the data and the results were recorded so that a maximum of useful information would be available for a comparative study of possible future amplifiers. It should also be noted that measurements were made on two "α amplifiers" over a period of over 9 months with no noticeable change in any characteristics.

SENSITIVITY

The accuracy and linearity of the sensitivity was essentially dependent upon the ability of the open loop amplifier to fit the necessary conditions of equation 16. These properties were of most importance in the use of feedback resistors up to 10^{10} ohms although certain useful information was obtained with the use of larger resistors. For feedback resistors up to 10^{10} ohms the method described in Appendix V was employed for the most exact test. However, the ease of the square wave method described in Appendix VI made its use very desirable although only the accuracy of the sensitivity was determined and that value was limited to the accuracy of the

UNCLASSIFIED
ORNL-LR-DWG. 56742

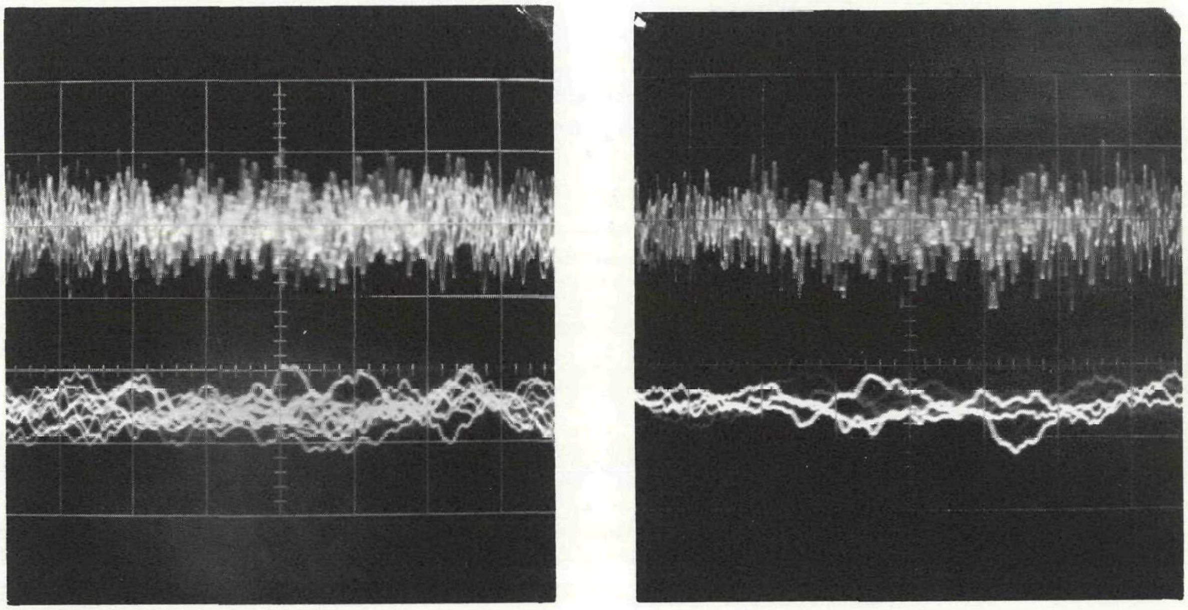

R = 10K Ω   C = 0.05μf
upper trace 100 mv/cm
lower trace 50 mv/cm
sweep 1m sec/cm

R = 10K Ω   C = 0.3μf
upper trace = 100 mv/cm
lower trace = 20 mv/cm
sweep = 2m sec/cm

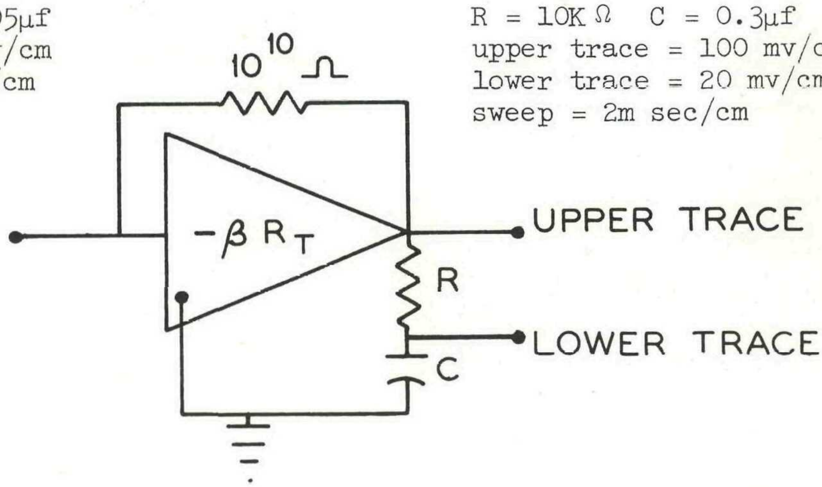

Fig. 25. Circuit Arrangement for Observing the a-c Noise of the "α Amplifier" with a Dual Beam Oscilloscope Along with Sample Traces

D-C DRIFT

Of primary importance in the actual usefulness of the amplifier was a study of the d-c drift characteristics. The observation of such drifts involved the measurement of the variation of the output voltage level with a sensitive voltmeter. Variations were referred to an equivalent input current in the usual manner using equation 23. The initial considerations involved measurements at fairly constant temperatures as encountered in the laboratory. Temperature change effects, however, were also studied and resulted in drifts that were typical of the temperature dependence of the collector to base current I_{cb}. Such a current flowing in the base circuit obviously could not be distinguished from an input current so that it contributed to the output voltage by the amount $I_{cb} R_f$. Due to the large current gain of Q_1, I_{cb} was probably the dominant factor in the drift characteristics. Some of the experiments involving this problem are described in Appendix VIII.

OUTPUT RESISTANCE

A final determination of the output resistance, R_o, following the previously mentioned definition of being the load resistance required to reduce the amplifier sensitivity in half, resulted in low values approximating those that would be expected from equation 42. A square wave was used for the test with a resistive load that was varied until the output amplitude was reduced to one half of the value that existed with no load. This simple method was sufficient to show that all of the resulting output resistances were very satisfactory.

PRESENTATION OF "α AMPLIFIER" DATA

Final evaluation of the characteristics that most accurately describe the "α amplifier" was made with the full use of the previously mentioned methods. The presentation of the data in Tables VIII and IX is categorized in terms of the testing method and first lists the feedback resistance since it was the variable that provided control of the sensitivity. To clarify the references to the test conditions, the symbols used refer to the test circuits of Figures 26 and 27. In Appendix IX an analysis of the data has been made to determine the equivalent amplifier parameters that have been used in the design criteria.

Since the noise and drift characteristics were the same in the two methods they are listed only once. Also, it was noted that there was a slow output fluctuation when the largest feedback resistors were used. This was, of course, superimposed on the d-c drift. This data, as pointed out in Appendix VIII, follows an effect due to the variation of I_{cb} of the input transistor that has been measured directly.

Reference to another amplifier that was designed to use feedback resistors as large as 10^8 ohms is made in Appendix X. The input transistor required for this application again exhibited current gains in the millimicroampere range but the amount of gain necessary was much less than that required in the "α amplifier". The characteristics of this amplifier showed an improvement over those of the amplifier of Figure 2 upon proper consideration of the a-c noise, response time, and d-c drift.

UNCLASSIFIED
ORNL-LR-DWG. 56743

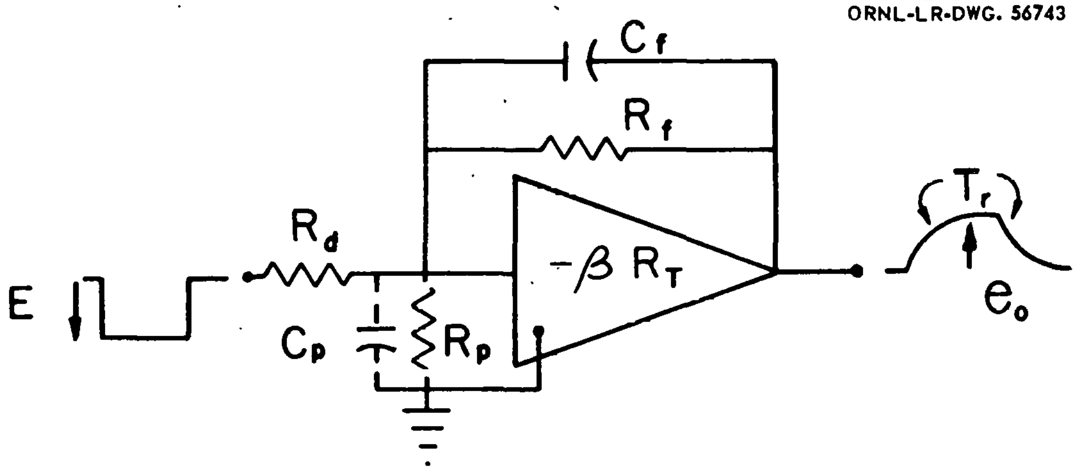

Fig. 26. Test Circuitry for Square Wave Analysis of "α Amplifier"

UNCLASSIFIED
ORNL-LR-DWG. 56744

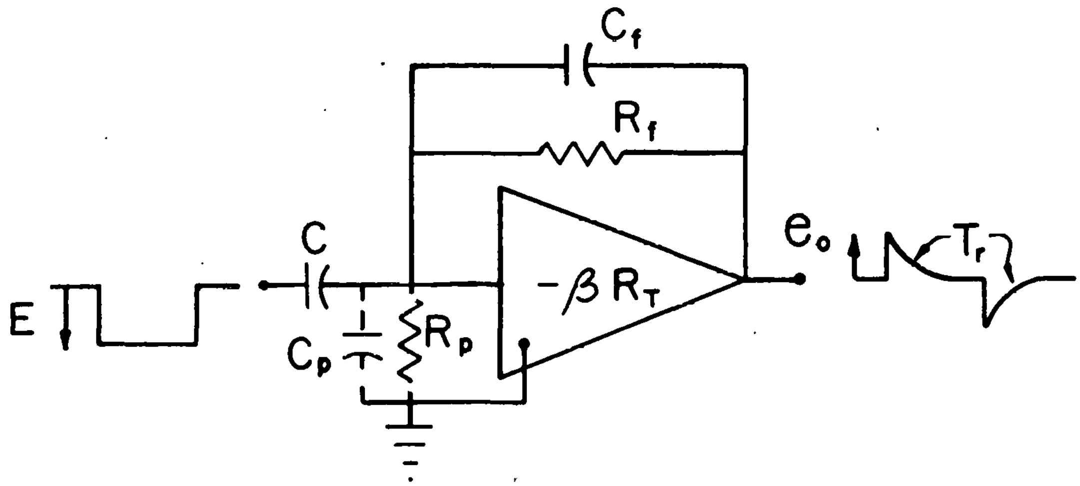

Fig. 27. Test Circuitry for Pulse Analysis of "α Amplifier"

CONCLUSION

The development of the low current "α amplifier" clearly pointed out how an unusual transistor effect was first noted and successfully incorporated into proper complementary circuitry to provide a very useful instrument. As a final result the "α amplifier" satisfactorily met-the specifications that were set up when conventional operation of commercial transistors had been pressed to the limit in the form of the amplifier of Figure 2.

The most complete description of the "α amplifier" follows directly from the data tabulated in Tables VIII and IX. For specific applications certain compromises could be made in terms of a-c noise, response time, and d-c drift so the data has been completed to the extent of allowing for rather easy determination of the feedback necessary for the appropriate use. Since the amplifier could be used with a wide range of feedback resistors a simple switching arrangement like the one shown in the amplifier of Figure 39 was incorporated in a final design that had sensitivities of $\frac{1}{10^{-8}}$, $\frac{1}{10^{-9}}$, and $\frac{1}{10^{-10}}$ $\frac{\text{volt}}{\text{amp}}$. This amplifier is pictured in Figure 28.

Due mainly to d-c drift considerations, operation with feedback resistors greater than 10^{10} ohms might be questioned in terms of any real overall improvement. However, applications involving the detection of low frequency signals occuring at the micro-microampere level probably would receive some enhancement with larger feedback resistors as long as the corresponding increased response time (decreased bandwidth) could be tolerated. The observed limit on detection of such signals has been due to the slight current fluctuation described in Appendix VIII.

The effect of temperature, specifically on the d-c drift, was not a major consideration in the original amplifier design mainly because of relatively constant temperature ambients. If this became a more significant consideration, temperature compensation would be necessary.

The analysis techniques employed throughout the development were most beneficial as a basis for design. The simple criteria derived from the basic concept of the input impedance and an equivalent amplifier forward loop transfer resistance (βR_T) was certainly directed toward transistor circuitry and clearly pointed out the ultimate limits that were afforded by the circuit arrangement.

Although the description of the "α amplifier" might be considered complete at this point, the improvement of its characteristics and the extension of its uses will continue as improved circuit components and techniques are developed. Also, transistors exhibiting the high gain effect will be utilized to the greatest possible benefit in future circuit development work.

Table VIII. Amplifier Characteristics Taken by the Square Wave Test Method Described in Appendix VI

R_f	Added C_f	Sensitivity	T_r	Output rms Noise Voltage	rms Noise Referred to a Current Input	d-c Drift Referred to a Current Input
ohms	μμf	$\frac{\text{volt}}{\text{amp}}$		mv	amp	$\frac{\text{amp}}{\text{min}}$
10^{12}	0	$\frac{0.95}{10^{-12}}$	100 ms	70	7×10^{-14}	$\frac{10^{-12}}{1}$
10^{12}	0.4	$\frac{0.95}{10^{-12}}$	500 ms	17	1.7×10^{-14}	$\frac{10^{-12}}{1}$
10^{11}	0	$\frac{1}{10^{-11}}$	7 ms	70	7×10^{-13}	$\frac{4 \times 10^{-13}}{1}$
10^{11}	0.4	$\frac{1}{10^{-11}}$	50 ms	7	7×10^{-14}	$\frac{4 \times 10^{-13}}{1}$
10^{10}	0	$\frac{1}{10^{-10}}$	500 μs	70	7×10^{-12}	$\frac{6 \times 10^{-12}}{40}$
10^{10}	0.4	$\frac{1}{10^{-10}}$	5 ms	7	7×10^{-13}	$\frac{6 \times 10^{-12}}{40}$
10^{9}	0.4	$\frac{1}{10^{-9}}$	500 μs	7	7×10^{-12}	$\frac{8 \times 10^{-12}}{10}$
10^{8}	0.4	$\frac{1}{10^{-8}}$	50 μs	7	7×10^{-11}	$\frac{4 \times 10^{-11}}{10}$
10^{7}	2	$\frac{1}{10^{-7}}$	20 μs	0.3	3×10^{-11}	$\frac{4 \times 10^{-10}}{15}$
10^{6}	5	$\frac{1}{10^{-6}}$	15 μs	0.3	3×10^{-10}	$\frac{2 \times 10^{-9}}{10}$
10^{5}	33	$\frac{1}{10^{-5}}$	5 μs	0.3	3×10^{-9}	$\frac{2 \times 10^{-8}}{10}$
10^{4}	430	$\frac{1}{10^{-4}}$	5 μs	0.3	3×10^{-8}	$\frac{2 \times 10^{-7}}{10}$
10^{3}	820	$\frac{1}{10^{-3}}$	2 μs	0.3	3×10^{-7}	$\frac{2 \times 10^{-6}}{10}$

Table IX. Amplifier Characteristics Taken by the Pulse Techniques Described in Appendix VII

R_f ohms	Added C_f $\mu\mu f$	C $\mu\mu f$	E volts	e_o volts	T_r ms
∞	0	0.025	2	8	9
10^{13}	0	0.025	4	2	800
10^{12}	0	0.025	5	2	100
10^{11}	0	0.025	8	3.9	7

UNCLASSIFIED
PHOTO 53255

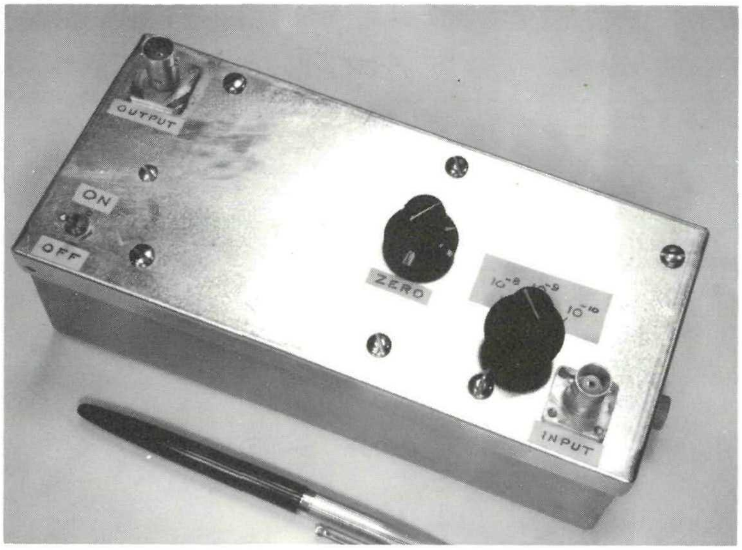

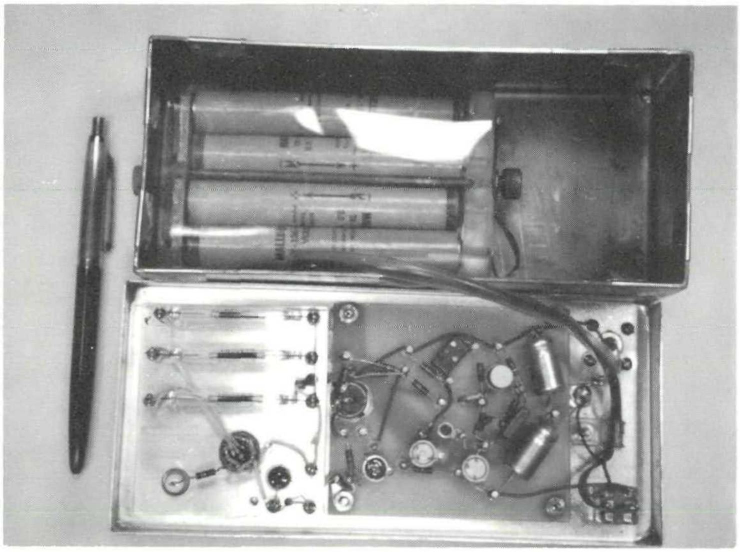

Fig. 28. "α Amplifier" with Switching for Sensitivities of $\frac{1}{10^{-8}}$, $\frac{1}{10^{-9}}$, and $\frac{1}{10^{-10}}$ $\frac{\text{volt}}{\text{amp}}$

REFERENCES

REFERENCES

1. SOME INTERESTING TRANSISTOR CHARACTERISTICS IN THE MILLIMICRO-AMPERE REGION, R. A. Dandl, F. T. May. The Review of Scientific Instruments, Vol. 31, no. 5, May, 1960, pp. 575-576.

2. THE ORNL THERMONUCLEAR PROGRAM, Sherwood Project, ORNL-2457, January 15, 1958.

3. THERMONUCLEAR PROJECT SEMIANNUAL REPORT FOR PERIOD ENDING JANUARY 31, 1959, ORNL-2693, May 5, 1959.

4. ON THE VARIATION OF JUNCTION-TRANSISTOR CURRENT-AMPLIFICATION FACTOR WITH EMITTER CURRENT, W. M. Webster, Proceedings of the IRE, September 3, 1953, pp. 914-920.

5. THE JUNCTION TRANSISTOR, (book) E. Wolfendale, The Macmillan Co., New York, 1958, pp. 76 and 95.

6. THE "HUSHED" TRANSISTOR AMPLIFIER, W. K. Volkers, N. E. Pedersen, Tele-Tech & Electronic Industries, Part One, December, 1955, pp. 82-84, pp. 156-158, Part Two, January, 1956, pp. 70-72, pp. 133-136, Part Three, pp. 72, 82, 129-136.

7. JUNCTION TRANSISTOR ELECTRONICS, (book) Richard B. Hurley, John Wiley & Sons, Inc., 1958, p. 14.

8. ELECTROMETERS AND AMPLIFIERS, Edward Fairstein, to be published in a "Handbook of Instruments and Techniques" by National Research Council Committee on Nuclear Science, pp. 24-26.

9. PRINCIPLES OF TRANSISTOR CIRCUITS, (book) R. F. Shea, John Wiley & Sons, Inc., 1953, p. 417.

10. GREATER GAIN BANDWIDTH IN TRIGGER CIRCUITS, Melvin Brown, RSI, March, 1959, Vol. 30, no. 3, pp. 169-175.

11. INTERNAL FEEDBACK AND NEUTRALIZATION OF TRANSISTOR AMPLIFIERS, A. P. Stern, C. A. Aldridge, and W. F. Chow, Proc. IRE, 1955, Vol. 43, pp. 838-847.

APPENDIXES

APPENDIX I. DATA ON SOME MESA TRANSISTORS

A brief presentation of data on some transistors of the mesa construction follows to illustrate the fact that interesting low current effects also exist to some extent in this different transistor geometry. This data were taken in the manner previously described. Table X lists the mesa transistors tested that exhibited any interesting characteristics below 10^{-8} amp of input base current. Figure 29 shows the best behavior of some of these types in the form of current gain vs. base current curves. These transistors have been incorporated into a current amplifier similar to the one described in Appendix X with some degree of success, mostly in terms of improved response time.

Since only a small number of mesas were tested no statistical information could be inferred as to the percentage of transistors with any current gain in the millimicroampere region that might be expected in an arbitrary order. Of course, in these transistors as in the other types mentioned one cannot at present expect these millimicroampere effects to be consistant from transistor to transistor since they have not been controlled in manufacture for this specific low current capability.

Table X. Data on Some si and ge Mesa Transistors Showing the Best Observed Values of Beta at Low Base Currents (V_{ce} = +1.0 volt)

Manufacturer	Type	Best Observed Test Values I_b	Best Observed Test Values Beta	Number Tested	Number of Interest
Texas Instruments	NPN si 2N696	5×10^{-10}	16	4	1
Texas Instruments	NPN si 2N702	5×10^{-11}	60		
		10^{-7}	8		
Texas Instruments	NPN ge 2N705	10^{-8}	20	4	1
		10^{-7}	30		
Transistron	NPN si 2N1139	5×10^{-10}	300	6	5
		10^{-8}	90		
Hughes Semiconductor	PNP si 2N1255	5×10^{-8}	5	3	3
		10^{-6}	18		
Hughes Semiconductor	PNP si 2N1257	5×10^{-8}	3	6	6
		10^{-6}	15		

UNCLASSIFIED
ORNL-LR-DWG. 56745

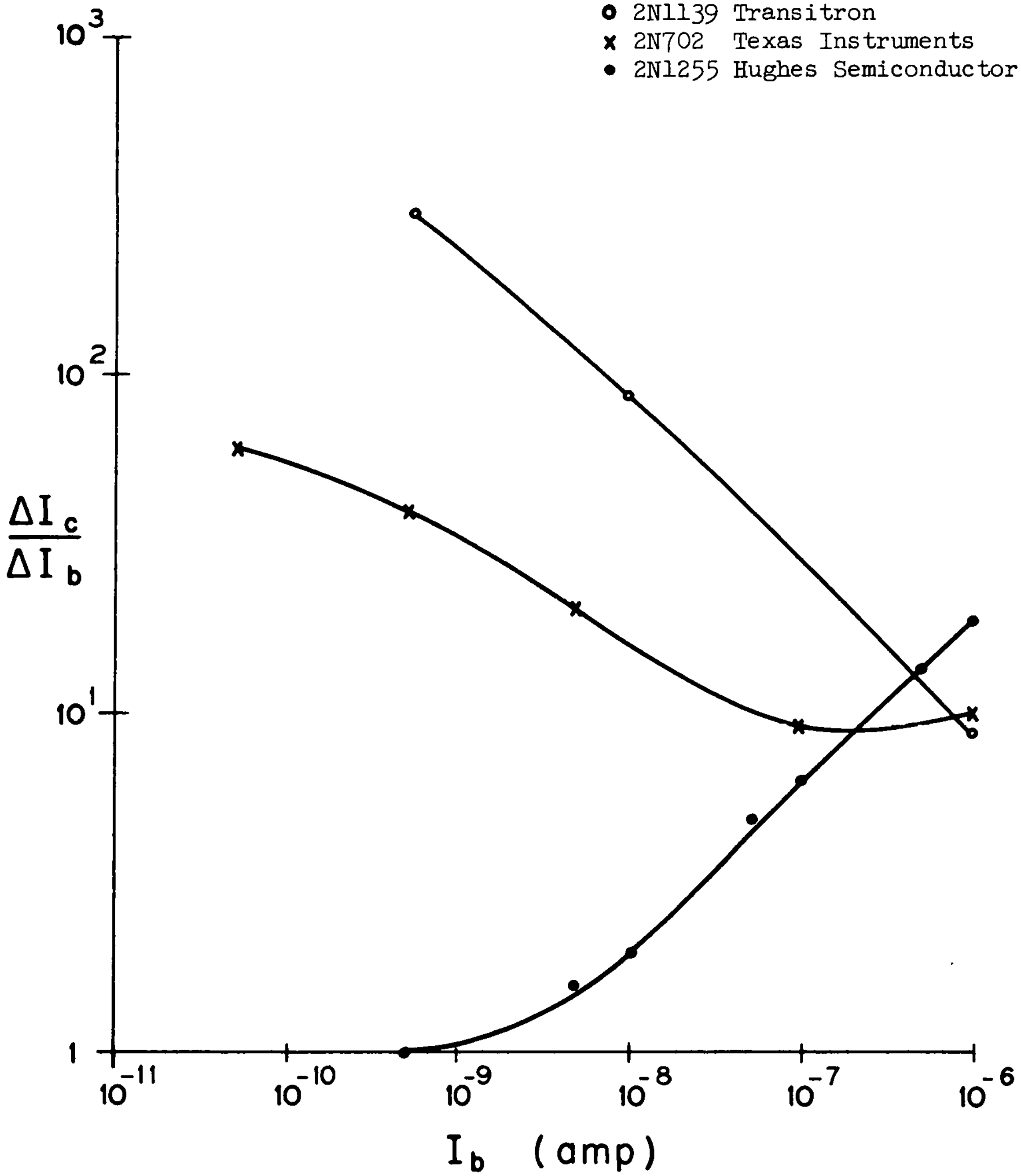

Fig. 29. Relation Between Beta and Base Current of Some Mesa Transistors

APPENDIX II. D-C INPUT RESISTANCE MEASUREMENT

One measurement of the input resistance utilized a simple procedure with a potentiometer and the special tester of Figure 3. The procedure was to first apply an emf, E_1, from the potentiometer to the "input through R_b" connector, with the normal I_b switch off using a large R_{b1} such as 10^{10} ohms chosen with the R_b switch. This would cause some particular collector current, I_{c1}, to flow. With these values noted, the base resistor was changed to R_{b2}, equal to $10^{-4} \times R_{b1}$, and the potentiometer voltage was changed to an E_2 which would yield a collector current, I_{c2}, equal to I_{c1}. Speaking in terms of the base currents being equal in the two cases due to the equal collector currents resulted in the relation

$$\frac{E_1 - V_{be}}{R_{b1}} = \frac{E_2 - V_{be}}{R_{b2}} \tag{26}$$

or

$$E_2 = \frac{R_{b2}}{R_{b1}} E_1 + V_{be} \left(1 - \frac{R_{b2}}{R_{b1}}\right) \tag{27}$$

This shows E_1 being reduced by 10^{-4} so that with E_1 of the order of one volt V_{be} need be only in the millivolt range to be the dominant term giving

$$E_2 \cong V_{be} \tag{28}$$

and, of course,

$$I_{b1} = \frac{E_1 - E_2}{R_{b1}} \tag{29}$$

Repeating this procedure beginning with another E_1', using the same values of R_{b1} and R_{b2}, gave another V_{be}' and I_b'. Then, by definition, the input resistance under these conditions of base current was

$$R_p = \frac{V_{be} - V_{be}'}{I_{b1} - I_{b1}'} = \frac{E_2 - E_2'}{E_1 - E_1 + E_2' - E_2} R_{b1} \qquad (30)$$

Making $(I_{b1} - I_{b1}')$ small compared to I_{b1} allowed this R_p to be associated with I_{b1}. Some data on the variation of input resistance with input current of two transistors are shown graphically in Figure 8.

APPENDIX III. CALCULATION OF FEDBACK OUTPUT RESISTANCE R_o'

R_o' was defined as the equivalent internal resistance presented in a Norton's equivalent circuit of the output of a shunt fedback current amplifier. From this definition the value of R_o' was calculated in terms of the load resistance necessary to reduce the gain of the amplifier to one half of the value that exists with an infinite load resistor.

From equation 14 the steady state output voltage was

$$e_o = \frac{\beta R_T I R_f}{R_f + R_p + \beta R_T} \tag{31}$$

An equivalent current gain, β_o, for the output circuit was defined to express R_T in terms of the open loop output resistance, R_o. By definition

$$\beta_o = \frac{e_o/R_o}{i_{b5}} \tag{32}$$

where e_o/R_o equals the equivalent output current and i_{b5} equals the input current of the output circuit. Then since $R_T = e_o/i_{b5}$

$$\beta_o = R_T/R_o \tag{33}$$

or

$$R_T = \beta_o R_o \tag{34}$$

Substituting equation 34 into 31 gave

$$e_o/I = \frac{\beta\beta_o R_o R_f}{R_f + R_p + \beta\beta_o R_o} \tag{35}$$

where $(\beta\beta_o)$ was the equivalent total current gain of the amplifier. This was the gain for an infinite load resistance. However, with a finite load, R_L, R_o was shunted by R_L giving a total load resistance

$$R_{LT} = \frac{R_o\ R_L}{R_o + R_L} \tag{36}$$

Then, by the 1/2 gain definition of R_o', substitution of R_{LT} for R_o gave

$$\frac{(\beta\ \beta_o)\ R_f\ \dfrac{R_L\ R_o}{R_L + R_o}}{R_f + R_p + \dfrac{(\beta\ \beta_o)\ R_L R_o}{R_o + R_L}} = 1/2\ \ \frac{\beta\ \beta_o\ R_o\ R_f}{R_f + R_p + \beta\ \beta_o\ R_o} \tag{37}$$

giving

$$\frac{2\ R_L}{(\beta\ \beta_o)\ R_o\ R_L + R_o\ R_f + R_o\ R_p + R_L\ R_f + R_L\ R_p} = \frac{1}{R_f + R_p + (\beta\beta_o)R_o} \tag{38}$$

or

$$R_L = \frac{(R_f + R_p)\ R_o}{R_f + R_p + (\beta\beta_o)\ R_o} \tag{39}$$

By the condition of equation 37

$$R_L = R_o' \tag{40}$$

$$R_o' = \frac{R_o}{1 + \dfrac{\beta R_T}{R_f + R_p}} \tag{41}$$

From the conditions necessary for useful operation, equation 16, this became

$$R_o' \cong \frac{R_o}{\beta R_T/(R_f + R_p)} \tag{42}$$

APPENDIX IV. OUTPUT CIRCUIT ANALYSIS

An approximate analysis of the output circuit has been made with reference to Figure 30. The main assumptions and definitions were:

1. $Beta_5 = Beta_6 =$ (by definition) $\beta_{5,6} \gg 1$
2. The transistors have sufficient collector resistance to be considered as current sources, $i_c = \beta_{5,6} i_b$
3. The input resistance, R_6, of Q_6 is essentially its common-emitter input resistance. A typical curve showing the variation of R_6 with I_c is shown in Figure 31 with the values of Beta also shown so that the parameters could easily be picked for calculations
4. Diode dynamic resistance, $R_d \ll r$ and R_6
5. The current, i_{b5}, into the base of Q_5 is driven from a source resistance much greater than the input resistance of Q_5.

The equations describing the action of the circuit were:

$$i_d = \beta_{5,6}\, i_{b5} - i_1 \tag{43}$$

$$e_o + (i_2 + i_d) R_6 + i_2 R = 0 \tag{44}$$

$$i_1 r - i_d R_d - (i_2 + i_d) R_6 = 0 \tag{45}$$

$$i_1 = \frac{e_o}{R_L} - \beta_{5,6}(i_d + i_2) \tag{46}$$

These four equations were rewritten as three equations suitable for a simple determinant analysis.

$$-e_o = i_2(R_6 + R) + i_{b5}(\beta_{5,6} R_6) + i_1(-R_6) \tag{47}$$

$$0 = i_2(-R_6) + i_{b5}(-\beta_{5,6}R_d - \beta_{5,6}R_6) + i_1(r + R_d + R_6) \qquad (48)$$

$$e_o = i_2(\beta_{5,6}R_L) + i_{b5}(\beta_{5,6}^2 R_L) + i_1(R_L - \beta_{5,6}R_L) \qquad (49)$$

Solving for i_{b5}, with the previously mentioned assumptions, gave

$$i_{b5} \cong e_o \quad \frac{R(r + R_6) + rR_6 + \beta_{5,6}R_L r}{\beta_{5,6}^2 \; R_L Rr} \qquad (50)$$

For R_L infinite this becomes

$$e_o \cong i_{b5}\beta_{5,6}R \qquad (51)$$

Then applying the 1/2 amplitude definition of output resistance, described in Appendix III, equation 52 was written from equations 50 and 51.

$$\frac{\beta_{5,6}^2 \; R_L Rr}{R(r + R_6) + rR_6 + \beta_{5,6}R_L r} = 1/2 \; \beta_{5,6}R \qquad (52)$$

This gave

$$R_L = \frac{R(r + R_6) + rR_6}{\beta_{5,6} \; r} \qquad (53)$$

By the condition of equation 52 $R_L = R_o$ so

$$R_o = \frac{1}{\beta_{5,6}} \quad (R + R_6 + \frac{R}{r} R_6) \qquad (54)$$

The values that were used in the output circuit were

$R = 39K\Omega$

R_6=6K Ω for collector current $\cong$ 1 milliampere

$r = 1K\Omega$

$\beta_{5,6} \cong 100$

Therefore, as a further approximation

$$R_o \cong \frac{R}{\beta_{5,6}} \left(\frac{R_6}{r}\right) \tag{55}$$

The above calculations were admittedly very presumptuous so equation 55 was used mainly as a guide to the experimental study of the output circuit. One main consideration along this line of thought came from the wide variation of R_6 with the collector current of Q_6. This variation is shown in Figure 31. Obviously any change in the d-c operating conditions had a definite effect on the output resistance. This was made apparent upon consideration of the actual d-c voltage drop maintained by the series diodes. Defining the voltage

$$e' = V_d - V_{be6} \tag{56}$$

where V_d = total diode voltage drops

V_{be6} = base-to-emitter voltage of Q_6

no-load collector current of Q_6 became

$$I_{c6} = e'/r \text{ (with quiescent } e_o \text{ at ground potential)} \tag{57}$$

Substituting in the value of r from equation 57 into equation 55 gave

$$R_o \cong \frac{R}{\beta_{5,6}} \left(\frac{R_6 I_{c6}}{e'}\right) \tag{58}$$

Equation 58 revealed the possibility of varying the output resistance by the selection of the dioded especially since any reasonable I_{c6} could be easily selected by the choice of r and e'. Also, due to the dependence of R_6 upon I_{c6}, the product of the two did not change very significantly over the current range of interest making e' a dominant term. Another slight variation came from the dependence of $\beta_{5,6}$ upon I_{c6}.

The other term of interest was R_T which followed directly from equation 51.

$$R_T = \frac{e_o}{i_{b5}} \cong \beta_{5,6} R \qquad (59)$$

for the condition of $R_L \gg R_o$.

UNCLASSIFIED
ORNL-LR-DWG. 56746

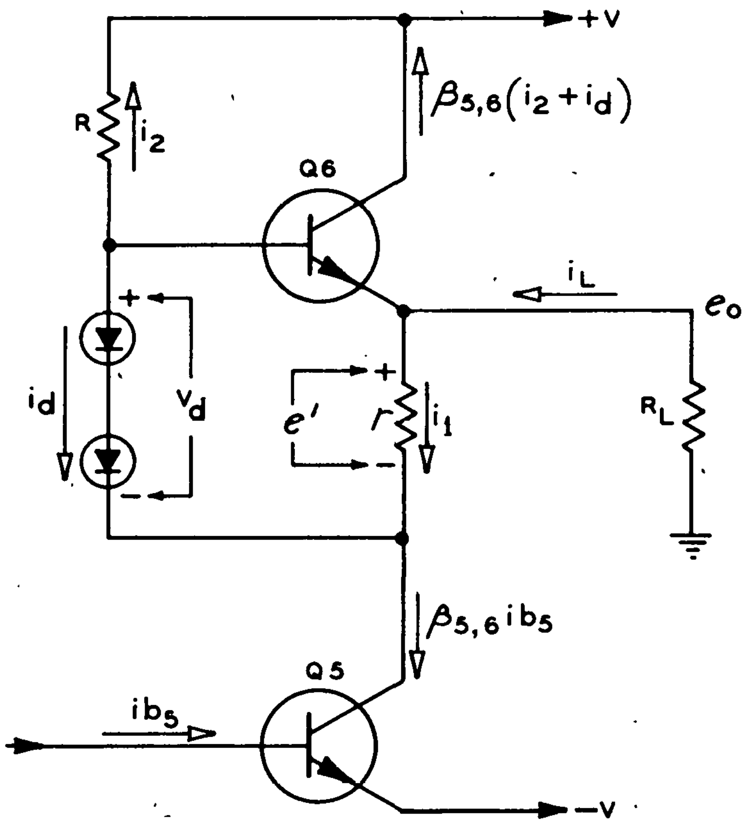

Fig. 30. Circuit for Analysis of "α Amplifier" Output

UNCLASSIFIED
ORNL-LR-DWG. 56747

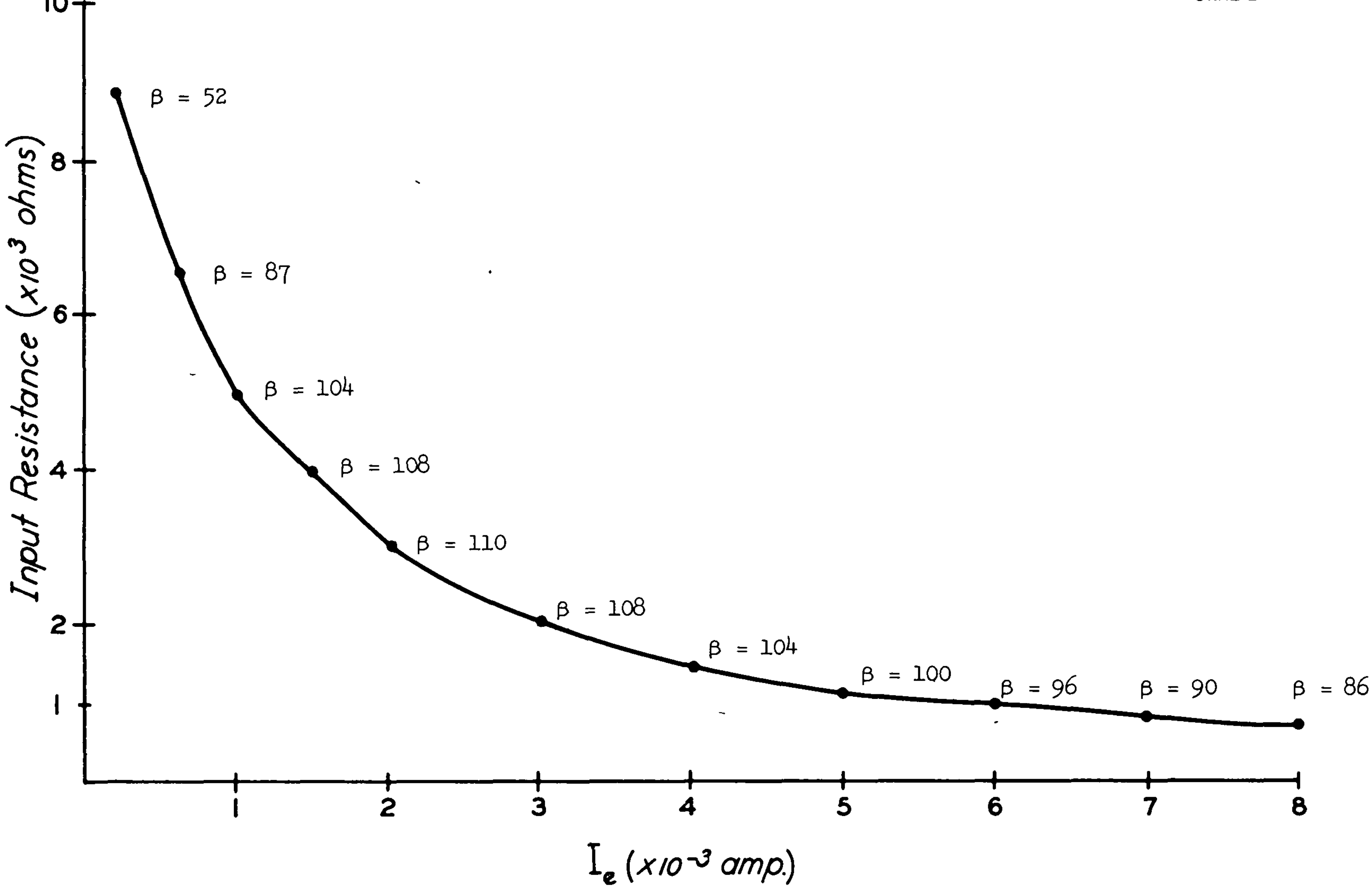

Fig. 31. Relation Between Input Resistance and Emitter Current of a 2N338 Operating at Normal Current Levels

APPENDIX V. ACCURACY AND LINEARITY TEST

One method of checking the accuracy and linearity of the amplifier sensitivity followed from the simple d-c test circuit of Figure 32. This method detected the output voltage error. The amplifier was first zeroed for a null out with both pots grounded. Then, with the two fixed d-c voltages of minus and plus 1.5V and plus and minus 15 volts accurately set, the two helipots were varied together. The voltmeter would read the amount by which the output was in error at any desired helipot settings. This method relied only upon the accuracy of the d-c voltages and the linearity of the helipots. The results of the tests on the amplifier showed that for all sensitivities checked (10^7 to 10^{10} ohms feedback) the linearity and the accuracy were within the experimental limits of the pot linearity (plus and minus 0.5%) and the feedback and driving resistors (plus and minus 1%) over the entire output dynamic range of plus and minus 15 volts.

UNCLASSIFIED
ORNL-LR-DWG. 56748

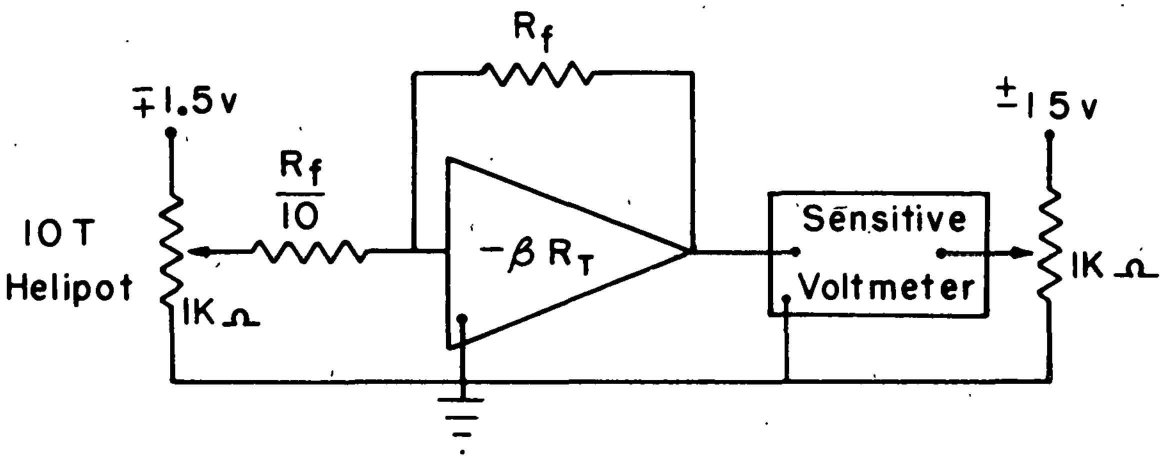

Fig. 32. Circuit for Checking the Accuracy and Linearity of the "α Amplifier"

APPENDIX VI. SQUARE WAVE TEST METHOD

The obvious straightforward test of the amplifier characteristics employed the standard square wave techniques, Figure 26. This clearly illustrated the fedback amplifier response to a step input. In this case the step was actually a voltage instead of the desired current. However, it can be shown by an analysis similar to the one used to derive equation 14 that with the necessary conditions of equation 16 satisfied the step appeared to the amplifier to be a current step of amplitude

$$I = E/R_d \tag{60}$$

The only added condition was that the intrinsic capacity, C_d, of R_d had to be small enough to allow the relation

$$R_d C_d \ll R_f C_f \tag{61}$$

to be met. The resulting output then followed equations 14 and 15 giving

$$-e_{o(t)} = (E/R_d)\; R_f\; (1 - \exp\; (- \frac{t}{T_r})) \tag{62}$$

where

$$T_r = R_f\; (C_f + \frac{R_p}{\beta R_T}\; C_p) \tag{63}$$

APPENDIX VII. AMPLIFIER RESPONSE BY PULSE TECHNIQUES

Another method of measuring amplifier response that was especially useful when very large feedback resistors were used followed from the analysis of Figure 33. The characteristic equations were

$$i_1 = (E - iR_p)SC \tag{64}$$

$$i_1 = i + iR_pSC_p + i\frac{R_p}{Z_f} - \frac{e_o}{Z_f} \tag{65}$$

$$-e_o = \beta iR_T \tag{66}$$

$$Z_f = \frac{R_f}{SR_fC_f + 1} \tag{67}$$

where S was the Laplace operator. Solution of these equations yielded

$$-e_o = \frac{ESC\ \beta R_T}{1 + \frac{R_p}{R_f} + \frac{\beta R_T}{R_f} + S(R_pC_p + \frac{R_p}{R_f}R_fC_f + \frac{\beta R_T}{R_f}R_fC_f + R_pC)} \tag{68}$$

with the necessary condition of

$$\beta R_T >> R_p + R_f \tag{69}$$

$$\beta R_T \gg R_1 \frac{C}{C_f} \tag{70}$$

$$C_p \gg C \tag{71}$$

the response of the amplifier to a step voltage of amplitude E was

$$e_{o(t)} = E\frac{C}{C_f + \frac{R_p}{\beta R_T}C_p} \left(\exp\frac{-t}{R_f(C_f + \frac{R_p}{\beta R_T}C_p)}\right) \tag{72}$$

Equation 72 allowed two measurements of the total capacitance, C_T, that determines the response time, equation 16, of the amplifier. This total capacitance was

$$C_T = C_f + \frac{R_p}{\beta R_T} C_p \tag{73}$$

The two measurements obviously came from the attenuation factor C/C_T and the fall time $R_f C_T$ since both C and R_f were known. This total capacitance, of course, also appeared in the square wave analysis of Appendix VI.

For $R_f = \infty$ and $C_f = o$, equation 68 became

$$-e_o = \frac{ESC\beta R_T}{1 + SR_p (C_p + C)} \tag{74}$$

and since $C \ll C_p$ the step response was

$$-e_{o(t)} \cong \frac{EC\beta R_T}{R_p C_p} \left(\exp \frac{-t}{R_p C_p}\right) \tag{75}$$

This fall time clearly gave a measurement of the input time constant $R_p C_p$ and then allowed a direct calculation of βR_T from the output pulse amplitude since E and C were known. Also it can be shown that with this unfedback condition the risetime of the pulse described by equation 75 was simply limited by the intrinsic risetime of the forward loop amplifier excluding the input R_p-C_p circuit so that other descriptive information could be obtained from this one test.

This technique, very basically speaking, applied an input charge of EC onto an equivalent capacitance C_e shunted by an equivalent resistance, R_e. In the fedback case $C_e = C_T = C_f + \frac{R_p}{\beta R_T} C_p, R_e = R_f$. In the unfedback case $C_e = C_p$, $R_e = R_p$. Some typical pulse data following equations 72 and 75 are shown in Figure 34.

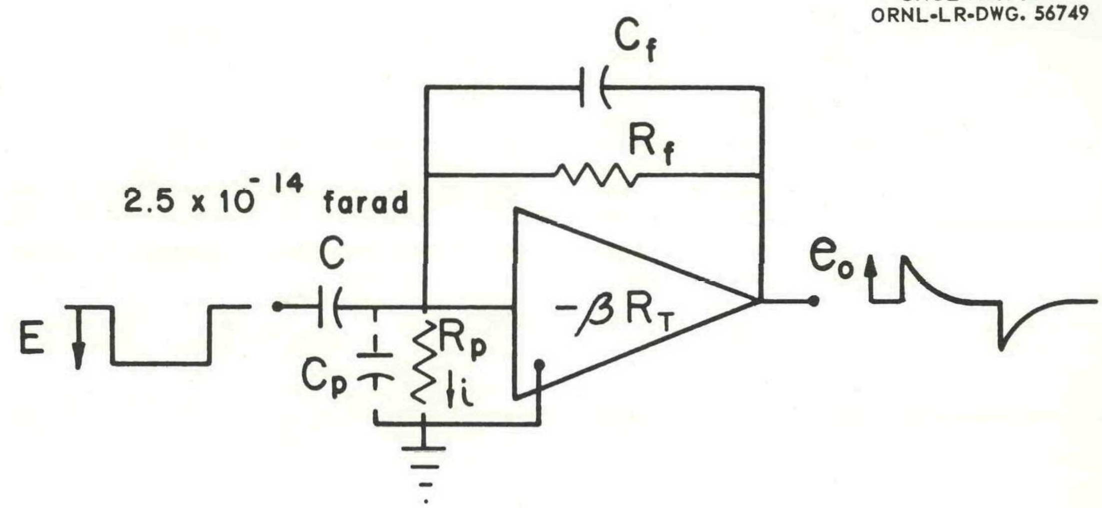

Fig. 33. Circuitry for Calculation of Amplifier Response by Pulse Techniques

UNCLASSIFIED
PHOTO 53256

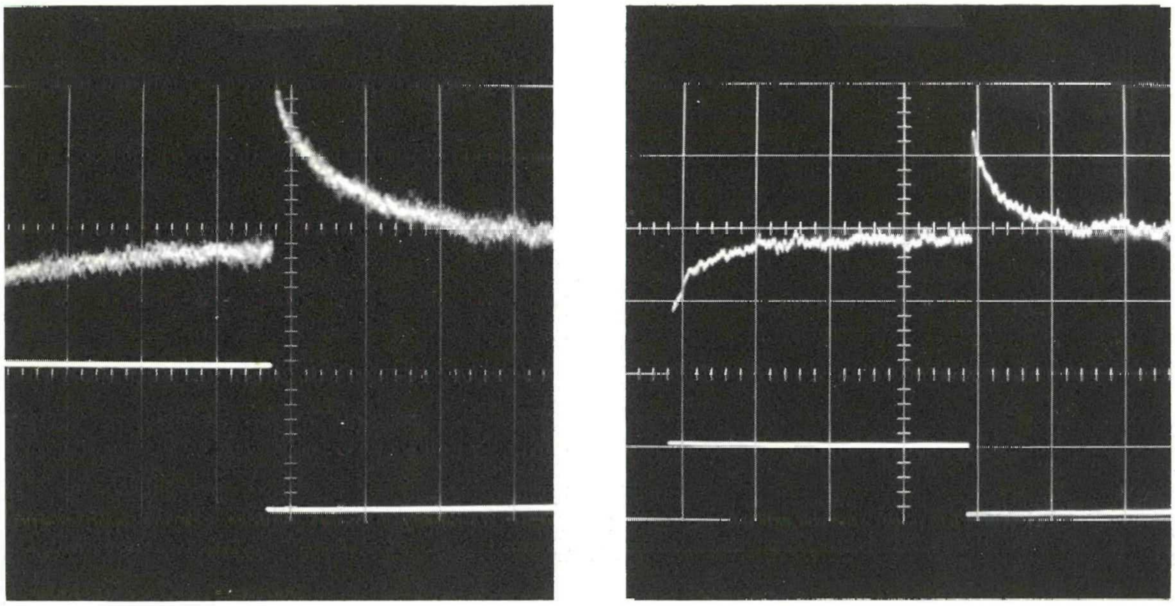

$R_f = 10^{11}$ ohms
e_o (upper trace) - $\frac{0.5\ v}{cm}$
E (lower trace) = $\frac{1v}{cm}$
dual sweep = $\frac{5m\ sec}{cm}$

$R_f = \infty$
e_o (upper trace) - $\frac{5v}{cm}$
E (lower trace) = $\frac{2v}{cm}$
dual sweep = $\frac{20m\ sec}{cm}$

Fig. 34. Typical Pulse Traces

APPENDIX VIII. DRIFT AND NOISE EXPERIMENTS

A number of experiments were performed to determine the character of the drift and noise of the "α amplifier" and the input transistor, Q_1. Some of the experiments are briefly described in this appendix.

The dependence of I_{cb} upon temperature is well known so no additional proof of its existance is really necessary. However, from the data of Figure 7 it is evident that the exponential nature of I_{ceo} can be easily referred to the input and be considered as an equivalent drift in the base circuit. From experiments involving the drift of the "α amplifier" under temperature variation this expected relation has also been noted. The curves shown in Figure 35 illustrate this behavior.

Another characteristic of the transistors suitable for use as Q_1 was not so much expected. This behavior was found experimentally to be a fluctuation of the equivalent input base current that proved to be a practical lower limit on the current that could be successfully detected. Observation of the fluctuation revealed irregular peaks occuring in a low-pass bandwidth with a peak-to-peak amplitude of about 5×10^{-13} amp. A number of experiments verified the existance of this form of noise. The methods of studying this basic problem are noted in Figures 36 and 37.

The observation of d-c drifts at room temperature also followed directly from the data in Table VIII and Figure 37, and of course was of prime importance. Another interesting study of d-c drift was made possible by the capacitively fedback circuit of Figure 38. The associated data were actually taken to determine the integral drift rate properties which depended on proper zeroing of the amplifier and was also dependent upon the leakage resistance, R_c of the feedback capacitor. However, an equivalent d-c drift current could be inferred by the simple relation

$$I_{d-c} = \frac{C_f V}{t} \qquad t \ll R_c C_f \cong 10^4 \text{ sec}$$

where

V = output voltage drift

t = observation time

This gave an average drift of approximately 0.83×10^{-12} amp in ten minutes.

UNCLASSIFIED
ORNL-LR-DWG. 56750

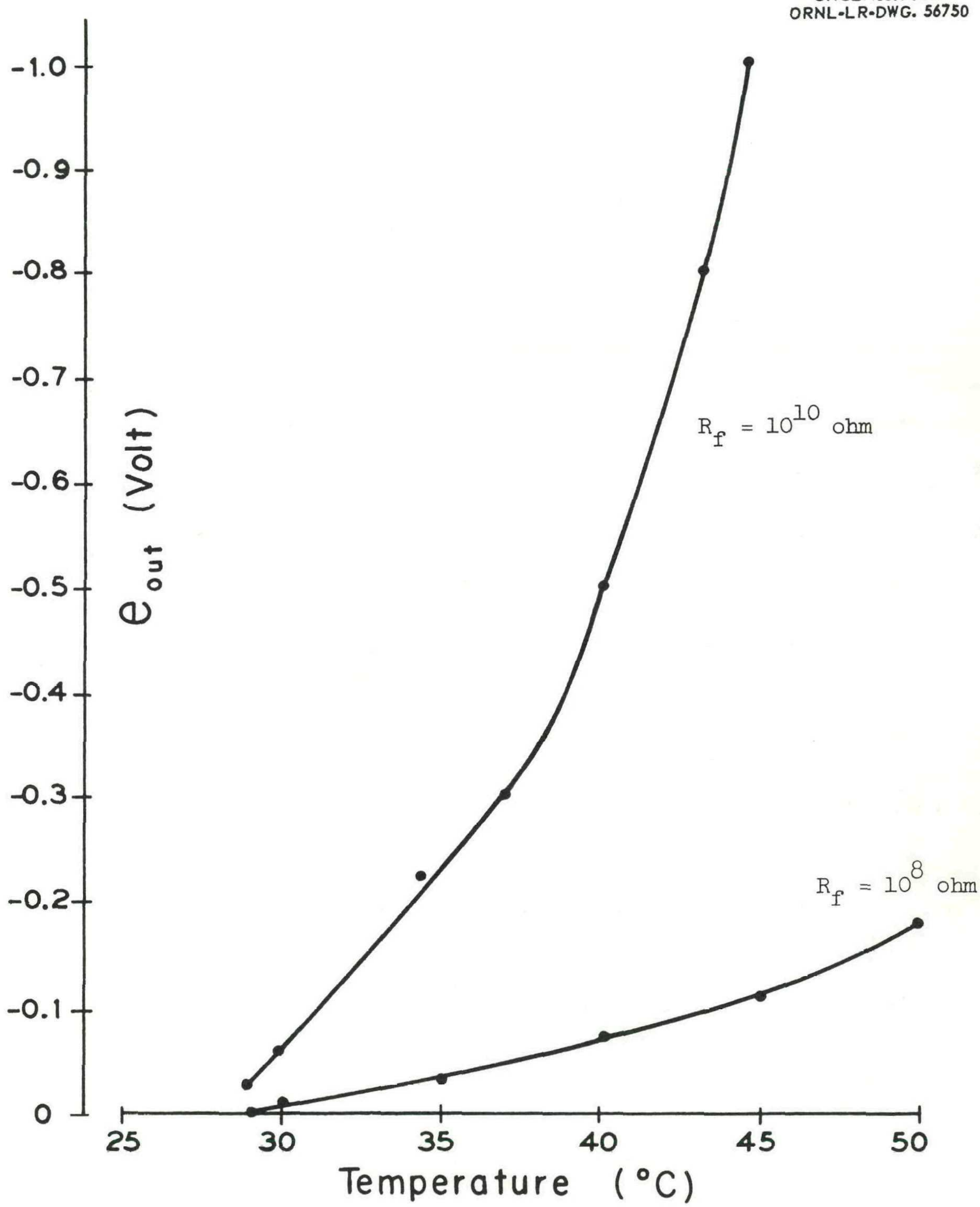

Fig. 35. Variation of Output Voltage With Temperature Under Two Conditions of Feedback

UNCLASSIFIED
PHOTO 53257

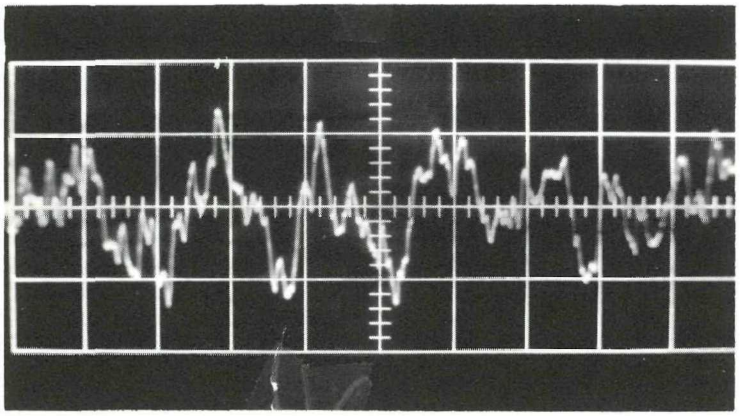

$R_f = 10^{10}$ ohms
Amplitude 2 mv/cm
Sweep 0.5 sec/cm

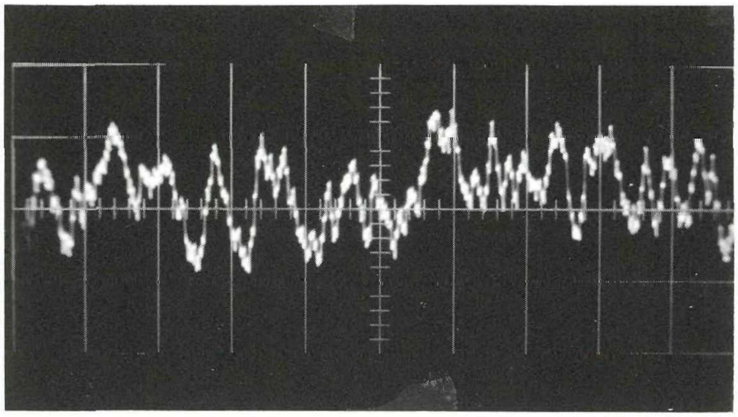

$R_f = 10^{9}$ ohms
Amplitude 0.2 mv/cm
Sweep 0.5 sec/cm

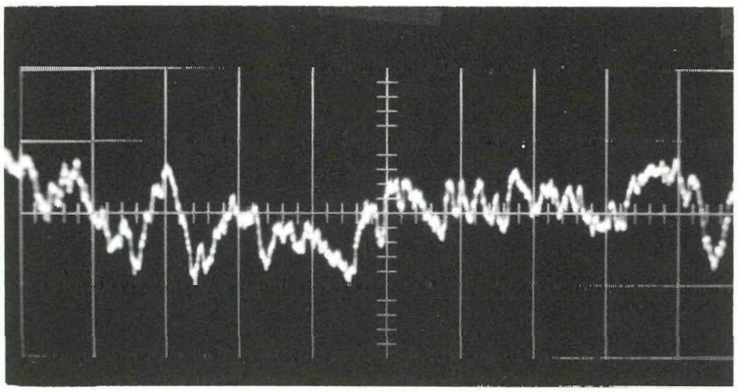

$R_f = 10^{8}$ ohms
Amplitude 0.05 mv/cm
Sweep 0.5 sec/cm

Fig. 36. Traces of the Output Noise Under Three Conditions of Feedback that Indicate a Slow Equivalent Input Current Noise of Approximately 5×10^{-13} amp Peak-to-Peak (Test Bandwidth 4 cps)

UNCLASSIFIED
ORNL-LR-DWG. 56751

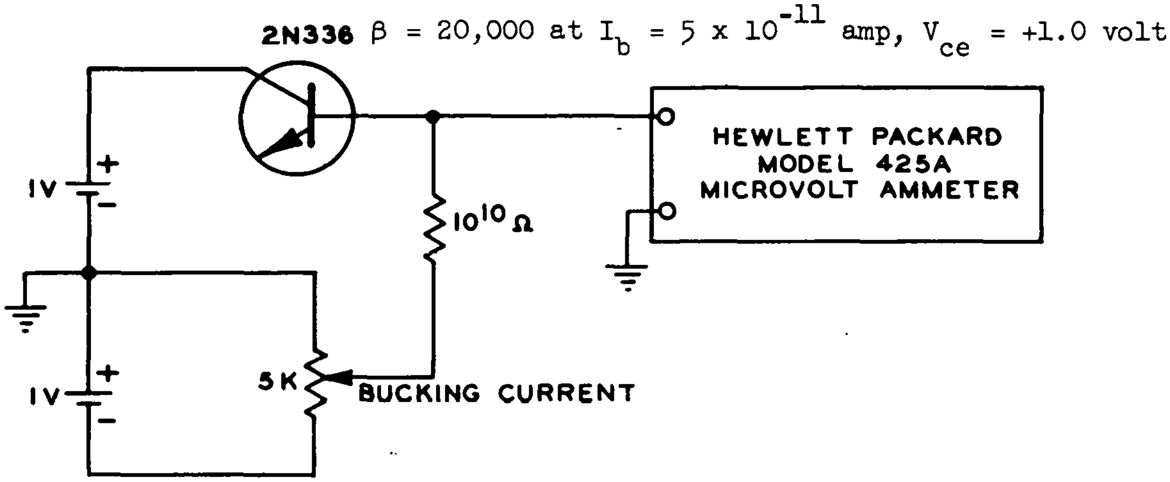

I_{cbo} = 4 x 10^{-11} amp, I_{ceo} = 3 x 10^{-7} amp

ΔI_{cbo} = 6 x 10^{-13} amp peak-to-peak

$$I_{cbo} \text{ drift} = \frac{2 \times 10^{-13} \text{ amp}}{5 \text{ min}}$$

Fig. 37. A Simple Circuit for Measuring Small Changes in the Collector-to-Base Current of a High Gain 2N336

UNCLASSIFIED
ORNL-LR-DWG. 56752

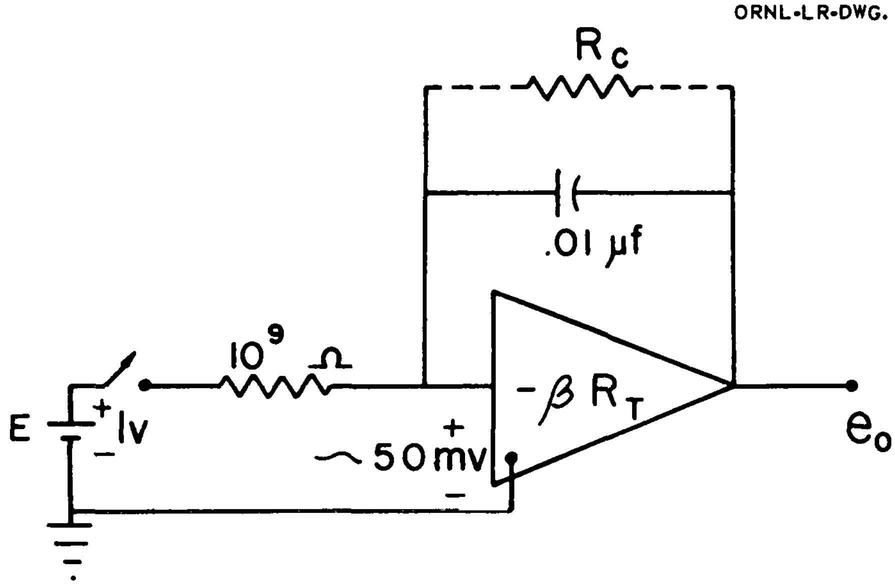

Fig. 38. Circuit for Measuring the Integral Drift Rate of the "α Amplifier" (data shown below)

Charging Measurement (E switch closed at t = 0)

time (sec)	e_o (volts)
0	+10.0
30	+ 7.05
90	+ 1.20
150	- 4.85
210	-10.6

Drift Measurement (E switch open)

time (sec)	e_o (mv)	equivalent drift µµ amp
0	-500	
300	-520	
600	-550	0.83
0	+500	
1500	+180	2.13

$I_{applied} = 9.5 \times 10^{-10}$ amp

$I_{calculated} = \frac{cv}{t} = 9.8 \times 10^{-10}$ amp

APPENDIX IX. ANALYSIS OF "α AMPLIFIER" DATA

From the data of Tables VIII and IX some calculations have been made to evaluate the basic parameters defined for the determination of a criteria for the initial amplifier design. These basic parameters being simply βR_T, R_p, and C_p. It should be kept in mind that previous measurements have shown these values to be functions of various current conditions so that variations in the analysis was expected. The true significance of this analysis, however, lies in the ability to show that the amplfier was designed to the point that a maximum usefulness was obtained from the chosen shunt fedback arrangement upon consideration of ultimate sensitivity and βR_T.

For example, the necessary condition of equation 16, which required that

$$\beta R_T >> R_f + R_p \tag{16}$$

for accuracy, apparently was fulfilled when $R_f = 10^{12}$ ohms. The square wave data suggested that under those feedback conditions βR_T was at least twenty times greater than 10^{12} ohms since the observable error was only five per cent. Therefore

$$\beta R_T \cong 2 \times 10^{13} \text{ ohms} \tag{77}$$

and since $R_T = 2 \times 10^6$ ohm

$$\beta \cong \frac{20 \times 10^{12}}{2 \times 10^6} = 10^7 \tag{78}$$

This value certainly was reasonable since

$$\beta = \beta_1 \, \beta_2 \, \beta_3 \, \alpha_4 \tag{79}$$

and β_1 for very low base currents was greater than 10^4.(The numerical subscripts refer to the respective transistors). This value of βR_T allowed for an evaluation of the amplifier characteristics down to the micro-microampere level of input currents proving its maximum usefulness. This statement refers to the reasonable accuracy noted with a sensitivity of 10^{-12} amp/volt which was all that could be of any use due to the intrinsic equivalent input current fluctuation approximately 5×10^{-13} amps described in Appendix VIII. The amplifier criteria clearly indicated the βR_T that would be necessary for such behavior and experimental observations revealed the basic limitation due to noise so that as a result the amplifier was pushed to the apparent limit of low current performance.

Calculations involving the assumed R_pC_p input circuit and the response characteristics showed some slight discrepancies. However, reasonable agreement followed from the amplifier pulse data with $R_f = \infty$ (Table IX) and from the dynamic input impedance measurements of the input transistor, Figure 9. The pulse data implied that R_pC_p = 9ms (refer also to Appendix VII) while the impedance measurements implied that $R_pC_p \cong 6 \times 10^7 \times .6 \times 10^{-10} = 3.6$ ms. These numbers agreed within a factor of 2.5 which spoke fairly well of the idea of using such a simple equivalent input circuit to evaluate the basic current action at the base of the input transistor.

A study of the basic response of the amplifier with finite feedback impedances involved mainly the defined total capacitance (refer to Appendix VII)

$$C_T = C_f + C_p \frac{R_p}{\beta R_T} \tag{73}$$

The response time has been analytically shown to be

$$T_r = R_f C_T \tag{16}$$

Typical calculations of C_T using the various methods previously described are shown in Table XI. All measurements were taken with no added feedback capacitance so that only geometrical shunt capacitance existed for C_f. Although this data varied as much as a factor of 2, there was enough agreement to say that

$$C_T \cong 0.07 \ \mu\mu f \tag{80}$$

Actual measurement of the effective shunt capacitance, C_f, of R_f as physically mounted in the circuit (with leads electrically moved only) by simple pulse techniques disclosed that

$$C_f \cong 0.013 \ \mu\mu f \tag{81}$$

Then from the definition of C_T

$$C_p \frac{R_p}{\beta R_T} = C_T - C_f \cong 0.057 \ \mu\mu f \tag{82}$$

However, calculation of this ratio from previous numbers yielded a maximum of

$$\frac{R_p C_p}{\beta R_T} \cong \frac{9 \times 10^{-3}}{2 \times 10^{13}} = 0.00045 \ \mu\mu f \tag{83}$$

which was different by 2 orders of magnitude from the other calculation. Analytically this seemed rather bad but a realization of the actual physical difficulty of having electrical circuitry with shunt capacities kept successfully below 0.1 μμf makes the problem more understandable. It was for this reason, of course, that the measurement of C_f was made with the resistor mounted in the circuit. The measured value of approximately 0.013 μμf fell short by a factor of five of being sufficiently large to account for the observed response time

The significance of these capacitance problems really was small in the actual amplifier application because of the a-c noise considerations. To reduce the output noise level from the intrinsic 200 mv level that existed with the large feedback resistors to a more satisfactory 20 mv level required an added feedback capacitance of approximately 0.4 μμf. The resulting effect of this capacitance made the contribution of C_T less than 20 per cent in the determination of the response time.

Further doubt on the completeness of the assumed equivalent input configuration was derived from other calculations of βR_T from the pulse amplitude data taken with $R_f = \infty$ and from output resistance, R_o', measurements. The resulting values of βR_T were as much as an order of magnitude below the most acceptable value of 2×10^{13} ohms.

Table XI. Calculated Values of C_T Using Experimental Data from the Square Wave and Pulse Methods

Test Method	R_f ohms	Calculated C_T $\mu\mu f$
Square Wave Rise Time	10^{12}	0.10
	10^{11}	0.07
	10^{10}	0.05
Pulse Fall Time	10^{13}	0.08
	10^{12}	0.10
	10^{11}	0.07
	10^{11}	0.075
Pulse Amplitude	10^{13}	0.05
	10^{12}	0.063
	10^{11}	0.05
	10^{11}	0.075

APPENDIX X. AN IMPROVED 10^{-8} AMP AMPLIFIER

Another current amplifier has been developed using techniques similar to those previously described. This amplifier is shown in Figure 39 with some typical characteristics in Table XII.

The major difference from the "α amplifier" was in the use of the input transistor, Q_1. The requirement on the current gain of Q_1 was

$$\frac{\Delta Ic}{\Delta Ib} \geq 200 \quad \text{at } I_b \cong 10^{-8} \text{ amp}$$

The statistics on the current gain variations of the Texas Instruments 2N336 transistors made this relatively easy to obtain. Biasing of the circuit was accomplished at the base of Q_1 so in this application the "floating base" condition was not approached.

Satisfactory operation of sensitivity switching was obtained using the switch arrangement shown in the feedback loop. This allowed for the grounding of the feedback impedances that were not in use. It was necessary to do this because normal switch capacitances would give added shunt capacitance producing an undesirable increase in the response time when the large feedback resistors were in use. Switching of this type has also been adapted for the "α amplifier".

The resulting characteristics indicate that better performance could be expected over the amplifier of Figure 2 which used a commercial input transistor specifically designed for low current applications.

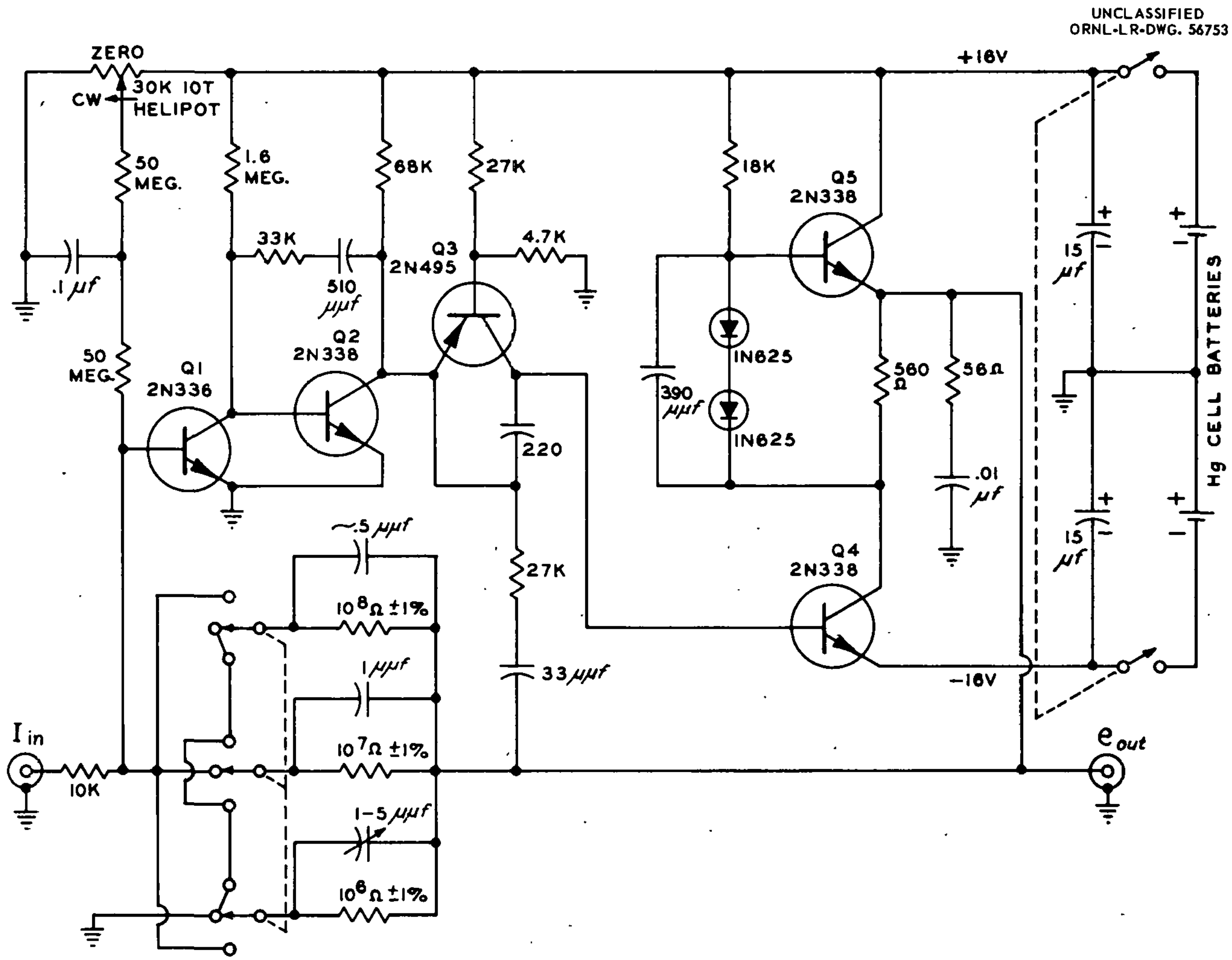

Fig. 39. An improved Amplifier With Sensitivities Extending Down to $\frac{1}{10^{-8}}$ $\frac{\text{volt}}{\text{amp}}$ Using a 2N336 for the Input Transistor

Table XII. Characteristics of the Amplifier Shown in Figure 39

R_f	Added C_f	Sensitivity	T_r	rms Noise Referred to a Current Input	d-c Drift Referred to a Current Input
ohms	$\mu\mu f$	$\frac{\text{volt}}{\text{amp}}$	μs	amp	$\frac{\text{amp}}{\text{min}}$
10^6	1 to 5	$\frac{1}{10^{-6}}$	4	7×10^{-10}	$\frac{4 \times 10^{-10}}{10}$
10^7	1	$\frac{1}{10^{-7}}$	12	1.7×10^{-10}	$\frac{5 \times 10^{-10}}{10}$
10^8	0.4	$\frac{1}{10^{-8}}$	50	3×10^{-11}	$\frac{4 \times 10^{-10}}{10}$
10^8	0	$\frac{1}{10^{-8}}$	25	7×10^{-11}	$\frac{4 \times 10^{-10}}{10}$

ORNL-3098
UC-37 – Instruments
TID-4500 (16th ed.)

INTERNAL DISTRIBUTION

1. I. Alexeff
2. R. G. Alsmiller
3. C. F. Barnett
4. M. C. Becker
5. P. R. Bell
6. L. L. Bennett
7. D. S. Billington
8. J. L. Blankenship
9. E. P. Blizard
10. C. W. Blue
11. C. J. Borkowski
12. G. E. Boyd
13. R. L. Brown
14. R. B. Burditt (Y-12)
15. C. E. Center (K-25)
16. R. A. Charpie
17. R. E. Clausing
18. J. W. Cleland
19. D. L. Coffey
20. F. L. Culler
21. J. S. Culver
22. O. L. Curtis
23. R. A. Dandl
24. J. B. Davidson
25. R. C. Davis
26. S. M. DeCamp
27. R. H. Dilworth
28. J. L. Dunlap
29. H. O. Eason
30. R. S. Edwards
31. T. L. Emmer
32. A. C. England
33. J. C. Ezell
34. R. J. Fox
35. J. L. Fowler
36. T. K. Fowler
37. J. E. Francis
38. J. H. Frye
39. W. F. Gauster
40. J. H. Gibbons
41. R. A. Gibbons
42. O. E. Gilcrease (Y-12)
43. F. M. Glass
44. A. A. Grau
45. P. M. Griffin
46. W. R. Grimes
47. E. Guth
48. C. S. Harrill
49. C. C. Harris
50. G. R. Haste
51. J. J. Henry (Y-12)
52. A. S. Householder
53. H. C. Hoy
54. W. J. Hulsey (Y-12)
55. R. P. Jernigan, Jr.
56. J. E. Jones
57. R. G. Jordan (Y-12)
58. W. H. Jordan
59. G. G. Kelley
60. M. T. Kelley
61. R. J. Kerr
62. R. L. Knight
63. P. Lafyatis
64. J. A. Lane
65. N. H. Lazar
66. G. F. Leichsenring
67. S. C. Lind
68. R. S. Livingston
69. J. L. Lovvorn
70. J. R. McNally, Jr.
71. R. J. Mackin
72. W. D. Manly
73. E. R. Mann
74. O. D. Matlock
75-94. F. T. May
95. B. J. Moore
96. K. Z. Morgan
97. O. B. Morgan
98. J. P. Murray (K-25)
99. R. V. Neidigh
100. J. H. Neiler
101. M. L. Nelson
102. J. Neufeld
103. C. E. Normand
104. G. R. North
105. C. E. Parker
106. W. F. Peed
107. J. F. Potts
108. M. Rankin
109. H. Postma
110. J. D. Redman
111. R. G. Reinhardt

112. M. T. Robinson
113. P. W. Rueff
114. W. K. Russell
115. H. E. Seagren
116. E. D. Shipley
117. A. Simon
118. M. R. Skidmore
119. M. J. Skinner
120. A. H. Snell
121. W. L. Stirling
122. R. F. Stratton, Jr.
123. R. A. Strehlow
124. J. A. Swartout
125. E. H. Taylor
126. A. Tell
127. P. A. Thompson
128. J. H. Todd
129. R. M. Warner
130. H. L. Watts
131. A. M. Weinberg
132. E. R. Wells
133. T. A. Welton
134. G. K. Werner
135. C. E. Winters
136. J. W. Woody
137. W. L. Wright
138. O. C. Yonts
139. W. P. Allis (consultant)
140. D. Alpert (consultant)
141. W. B. Ard, Jr. (consultant)
142. J. F. Bailey (consultant)
143. W. H. Bostic (consultant)
144. W. R. Chambers (consultant)
145. E. Creutz (consultant)
146. E. Fairstein (consultant)
147. J. W. Flowers (consultant)
148. M. W. Garrett (consultant)
149. O. G. Harrold (consultant)
150. E. G. Harris (consultant)
151. R. Hefferlin (consultant)
152. D. E. Harrison (consultant)
153. G. W. Hoffman (consultant)
154. V. W. Hughes (consultant)
155. D. W. Kerst (consultant)
156. E. D. Klema (consultant)
157. G. B. Lockhart (consultant)
158. E. W. McDaniel (consultant)
159. M. R. C. McDowell (consultant)
160. J. E. Mott (consultant)
161. H. Mott-Smith (consultant)
162. W. B. Pardo (consultant)
163. J. F. Pierce (consultant)
164. H. K. Reynolds (consultant)
165. F. F. Rieke (consultant)
166. H. S. Robertson (consultant)
167. D. J. Rose (consultant)
168. L. P. Smith (consultant)
169. H. S. Snyder (consultant)
170. P. M. Stier (consultant)
171. C. H. Weaver (consultant)
172. J. D. Tillman (consultant)
173. Thermonuclear Library
174. Sherwood Reading File (V. Glidewell)
175. Reactor Division Library
176-177. Central Research Library
178-197. Laboratory Records Department
198. Laboratory Records, ORNL R.C.
199. ORNL – Y-12 Technical Library, Document Reference Section

EXTERNAL DISTRIBUTION

200. E. P. Gyftopoulos, MIT
201. S. C. Brown, MIT
202. M. B. Gottlieb, Princeton University
203. J. M. B. Kellog, Los Alamos
204. A. C. Kolb, NRL
205. J. A. Phillips, Los Alamos
206. R. F. Post, LRL
207. Lyman Spitzer, Jr., Princeton University
208. E. Teller, University of California
209. C. M. Van Atta, LRL
210-211. Division of Research and Development, AEC, ORO (1 copy each to H. M. Roth and R. B. Martin)
212-213. Controlled Thermonuclear Branch, AEC, Washington (1 copy each to A. E. Ruark and H. S. Morton)
214. Oak Ridge Operations Office
215-851. Given distribution as shown in TID-4500 (16th ed.) under Instruments category (100 copies - OTS)